REPORT DOCUMENTATION PAGE

READ INSTRUCTIONS BEFORE COMPLETING FORM

1. REPORT NUMBER: SYRU/DECE/TR-85/1

2. GOVT ACCESSION NO.:

3. RECIPIENT'S CATALOG NUMBER:

4. TITLE (and Subtitle): CHARACTERISTIC MODES FOR SLOTS IN A GROUND PLANE TE CASE

5. TYPE OF REPORT & PERIOD COVERED: Technical Report No. 1

6. PERFORMING ORG. REPORT NUMBER:

7. AUTHOR(s):
Karim Y. Kabalan
Hesham A. Auda
Roger F. Harrington
Joseph R. Mautz

8. CONTRACT OR GRANT NUMBER(s): N00014-85-K-0082

9. PERFORMING ORGANIZATION NAME AND ADDRESS:
Dept. of Electrical & Computer Engineering
Syracuse University
Syracuse, New York 13210

10. PROGRAM ELEMENT, PROJECT, TASK AREA & WORK UNIT NUMBERS:

11. CONTROLLING OFFICE NAME AND ADDRESS:
Department of the Navy
Office of Naval Research
Arlington, Virginia 22217

12. REPORT DATE: May 1985

13. NUMBER OF PAGES: 82

14. MONITORING AGENCY NAME & ADDRESS (if different from Controlling Office):

15. SECURITY CLASS. (of this report): UNCLASSIFIED

15a. DECLASSIFICATION/DOWNGRADING SCHEDULE:

16. DISTRIBUTION STATEMENT (of this Report):

Approved for public release; distributed unlimited.

17. DISTRIBUTION STATEMENT (of the abstract entered in Block 20, if different from Report):

18. SUPPLEMENTARY NOTES:
This work was supported in part by a grant provided by the Committee on Faculty Research of the University of Mississippi

19. KEY WORDS (Continue on reverse side if necessary and identify by block number):
Aperture admittance
Characteristic Modes
Slot
TE excitation

20. ABSTRACT (Continue on reverse side if necessary and identify by block number):

Consider an infinitely long slot in a ground plane in an unbounded medium illuminated by a uniform TE (to the slot axis) plane wave. The theory of characteristic modes for slots is applied for solution of the problem. The characteristic currents and fields, as well as the equivalent magnetic current, transmission coefficient, and transmitted field pattern, of the slot are computed for different slot widths. Analytic expressions for the special case of a narrow slow are also given.

SYRU/DECE/TR-85/1

CHARACTERISTIC MODES FOR SLOTS IN A GROUND PLANE

TE CASE

by

Karim Y. Kabalan
Roger F. Harrington
Hesham A. Auda
Joseph R. Mautz

Department of
Electrical and Computer Engineering
Syracuse University
Syracuse, New York 13210

Technical Report No. 1

May 1985

Contract No. N00014-85-K-0082

Approved for public release; distributed unlimited

Prepared for

DEPARTMENT OF THE NAVY
OFFICE OF NAVAL RESEARCH
ARLINGTON, VIRGINIA 22217

SYRU/DECE/TR-85/1

CHARACTERISTIC MODES FOR SLOTS IN A GROUND PLANE

TE CASE

by

Karim Y. Kabalan
Roger F. Harrington
Hesham A. Auda
Joseph R. Mautz

Department of
Electrical and Computer Engineering
Syracuse University
Syracuse, New York 13210

Technical Report No. 1

May 1985

Contract No. N00014-85-K-0082

Approved for public release; distributed unlimited

Prepared for

DEPARTMENT OF THE NAVY
OFFICE OF NAVAL RESEARCH
ARLINGTON, VIRGINIA 22217

TABLE OF CONTENTS

1. Introduction

The problem of electromagnetic coupling from one region to another region through an aperture in a ground plane can be formulated in terms of two admittance operators, one for each region [1]. These admittance operators are complex and symmetric. Recently, a theory for the characteristic modes for apertures has been proposed [2]. These modes are defined as the eigenfunctions of a certain generalized eigenvalue equation involving the admittance operators and their real parts. Because of the particular choice of the eigenvalue equation, the characteristic modes are real (or equi-phasal) and orthogonal with respect to both the admittance operators, their real parts, and their imaginary parts over the slot. Furthermore, the characteristic fields produced by the characteristic modes are orthogonal over the radiation sphere. For small apertures, the characteristic mode theory reduces to an augmented Bethe hole theory, i.e., the aperture is described by a susceptance term related to the polarizability, plus a conductance term.

In this paper, the general theory is specialized to an infinitely long slot in a ground plane in an unbounded medium. The purpose of the paper is to illustrate the theory, then apply it for a complete analysis of the slot problem when the slot is illuminated by a uniform TE (to the slot axis) plane wave. Specifically, the characteristic currents and fields are computed for different slot widths. These are then used to compute the quantities and parameters of importance usually encountered in electromagnetic field compatibility problems, such as the equivalent magnetic current of the slot, transmission coefficient, and transmitted field pattern both near to and far from the slot. Analytic expressions for the special case of the narrow slot are also given.

The infinitely long slot problem has been extensively considered by researchers over the years. A long list of previous work can be found in [3] and [4]. The theory of characteristic modes is seen in this paper to be both general and computationally efficient. The extensions of the work here to a slot in a ground plane separating contrasting mediums, and to a uniform TM plane wave excitation of the slot are under preparation.

2. Basic Formulation

Let the excitation be a plane wave of unit amplitude incident on the slot at an angle θ from the left of the screen (see Figure 1). This wave is assumed to be uniform and TE to the slot axis, and therefore has the field distribution

$$\left.\begin{aligned} \underline{E}^i &= \zeta \left\{\cos\theta\, \underline{x} - \sin\theta\, \underline{z}\right\} e^{-j\kappa(x \sin\theta + z \cos\theta)} \\ \underline{H}^i &= e^{-j\kappa(x \sin\theta + z \cos\theta)} \underline{y} \end{aligned}\right\} \tag{1}$$

where

$$\left.\begin{aligned} \kappa &= \omega \sqrt{\mu\varepsilon} \\ \zeta &= \frac{\kappa}{\omega\varepsilon} \end{aligned}\right\} \tag{2}$$

are the medium wave number and impedance, respectively.

Because of the presence of the slot, part of the incident field is reflected back into the $z<0$ half-space, while the rest of it is transmitted through into the $z>0$ half-space. The total field, incident plus

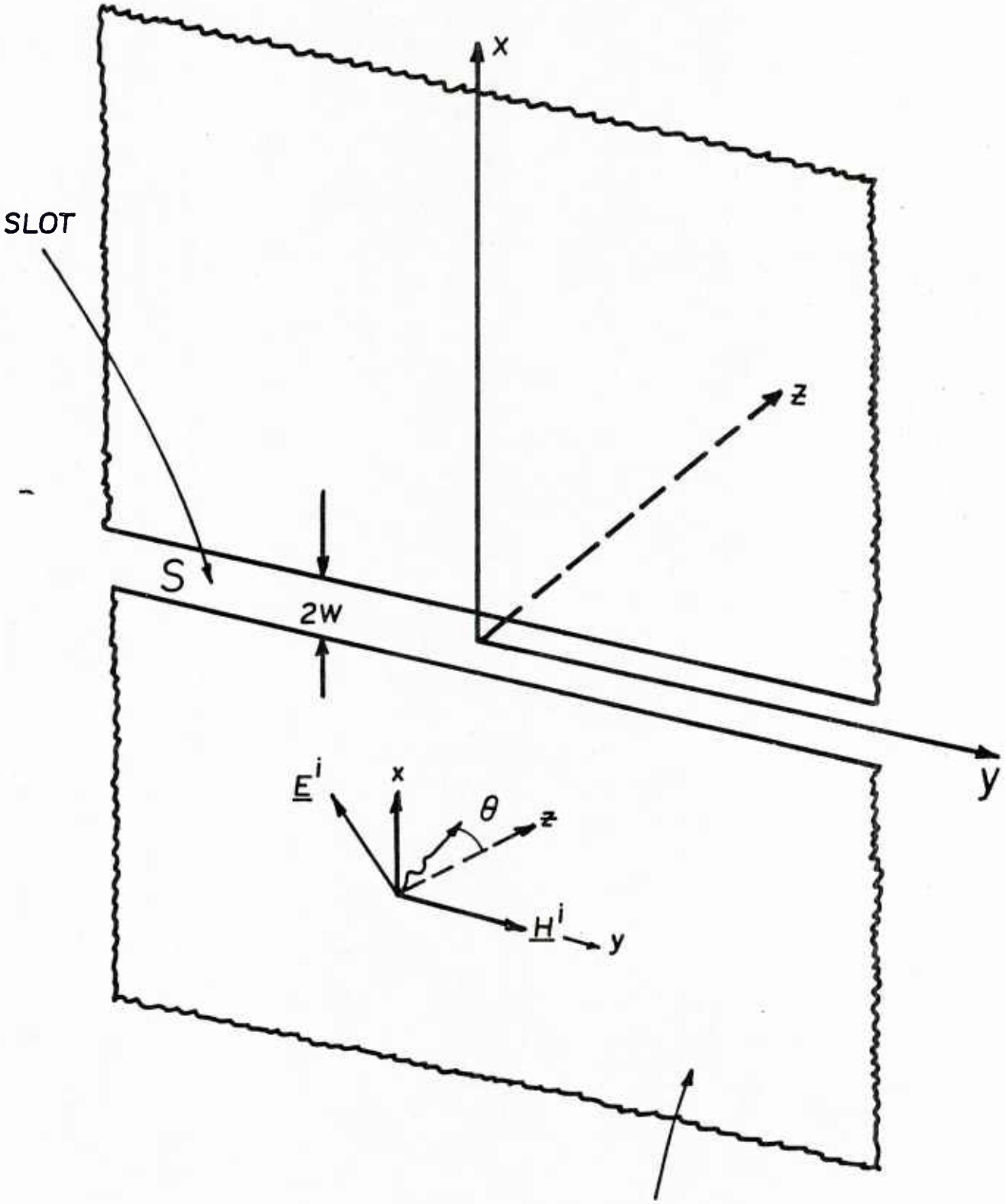

FIG. 1

AN INFINITELY LONG SLOT IN A GROUND PLANE

scattered, ($\underline{E}$, $\underline{H}$), must have zero electric field component tangent to the screen, and continuous tangential electric and magnetic fields across the slot. A field equivalence theorem is used to divide the problem into two decoupled parts.

Let the exciting field be incident while the slot is covered by a perfect conductor. This field, often referred to as the short circuit field ($\underline{E}^{sc}$, $\underline{H}^{sc}$), is given by

$$\left.\begin{aligned} \underline{E}^{sc} &= -2\zeta \left\{ j\cos\theta \sin(\kappa z \cos\theta)\, \underline{x} + \sin\theta \cos(\kappa z \cos\theta)\, \underline{z} \right\} e^{-j\kappa x \sin\theta} \\ \underline{H}^{sc} &= 2 \cos(\kappa z \cos\theta)\, e^{-j\kappa x \sin\theta}\, \underline{y}. \end{aligned}\right\} \tag{3}$$

By the field equivalence theorem [5, Section 3-5], the field to the left of the screen is identical with ($\underline{E}^{sc}$, $\underline{H}^{sc}$) plus the field ($\underline{E}(\underline{M})$, $\underline{H}(\underline{M})$) produced by the magnetic current sheet

$$\underline{M} = \underline{z} \times \underline{E} \Big|_{z=0} \tag{4}$$

on the slot while it is covered by a perfect conductor. The field to the right of the screen is then identical with the field ($\underline{E}(-\underline{M})$, $\underline{H}(-\underline{M})$) produced by the magnetic current sheet $-\underline{M}$ on the slot while it is covered by a perfect conductor. Figure 2 shows the equivalent situations.

Since the slot is uniform along the y-axis, and since the incident field has only an H_y component that does not vary with y, so does the scattered field. Thus, the total field is uniform and TE to the y-axis, and, as follows from (4), $\underline{M}$ has only a y-component that does not vary with y:

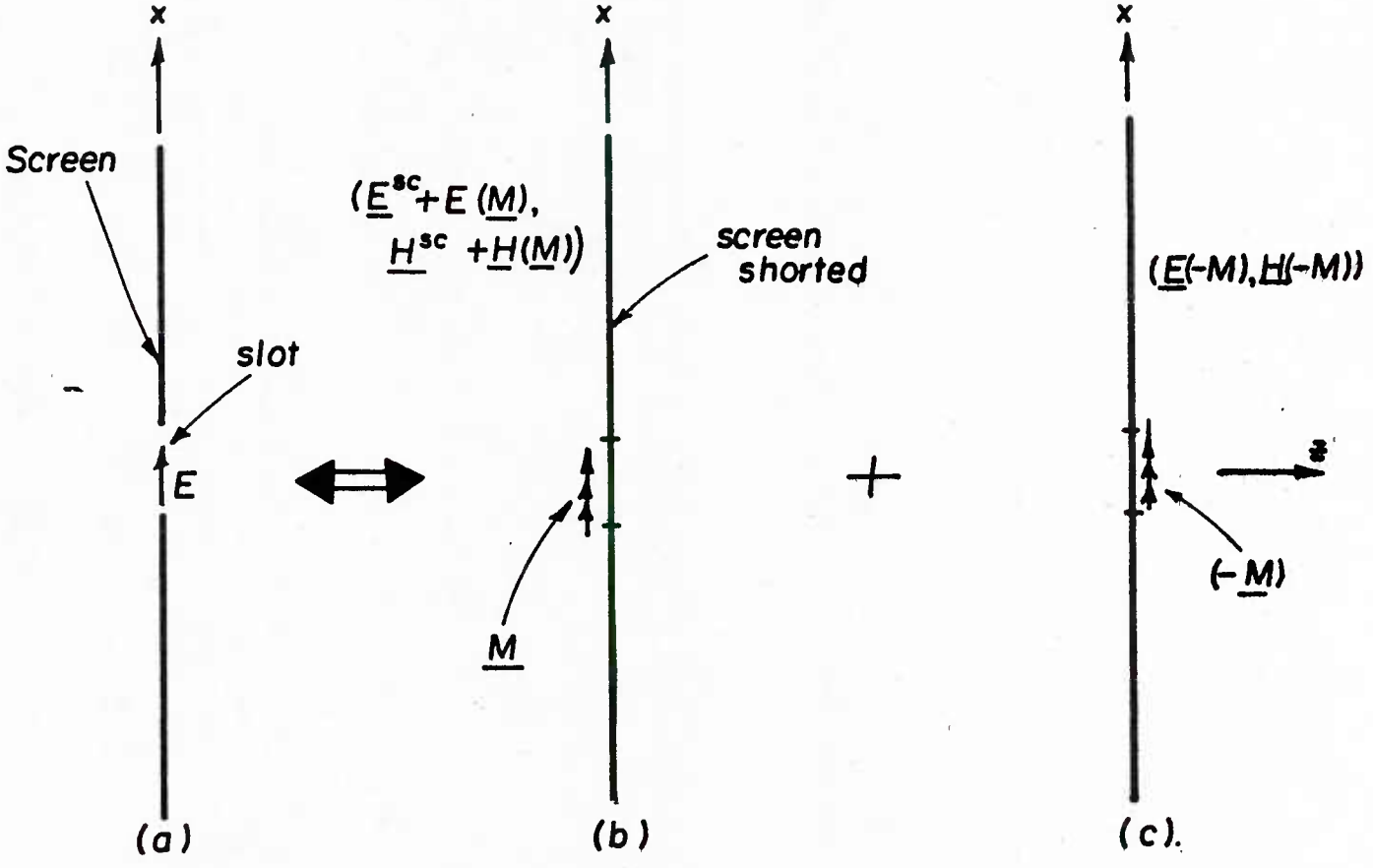

FIG. 2

THE EQUIVALENT SITUATIONS

$$\underline{M} = M(x)\ \underline{y}. \tag{5}$$

The field produced by $\underline{M}$ to the left of the screen is then given by [5, Section 3-12]

$$\left.\begin{aligned} \underline{E}(\underline{M}) &= -\nabla \times \underline{F}(\underline{M}) \\ \underline{H}(\underline{M}) &= -j\,\frac{\kappa}{\zeta}\,\underline{F}(\underline{M}) \end{aligned}\right\} \tag{6}$$

where $\underline{F}(\underline{M})$ is the electric vector potential produced by $\underline{M}$ in the presence of the complete screen [5, Section 5-7]:

$$\underline{F}(\underline{M}) = \left\{\frac{1}{j2}\int_{-w}^{w} M(x')\, H_0^{(2)}\left(\kappa\sqrt{z^2 + (x-x')^2}\right) dx'\right\} \underline{y}. \tag{7}$$

Here $H_0^{(2)}$ is the Hankel function of the second kind and zero order. Because of the linearity of the electric vector potential, the field produced by $-\underline{M}$ to the right of the screen is negative of that in (6).

The total tangential electric field clearly vanishes at the conducting screen. Furthermore, the tangential electric field is continuous across the slot by virtue of placing magnetic current sheets of opposite signs on the opposite sides of the slot. The continuity of the tangential magnetic field across the slot, however, requires that

$$\frac{\kappa}{\zeta}\int_{-w}^{w} M(x')\, H_0^{(2)}(\kappa|x-x'|)\, dx' = 2\, e^{-j\kappa x \sin\theta}, \qquad x \varepsilon S \tag{8}$$

as readily follows from (3), (6), and (7).

In the next section, the characteristic currents of the slot are defined. These are then utilized to solve (8) for M.

3. The Characteristic Currents of the Slot

The integral equation (8) can be put in the operator form

$$Y(M) = I \tag{9}$$

where

$$\left.\begin{aligned} Y(M) &= \frac{\kappa}{\zeta} \int_{-w}^{w} M(x')\, H_0^{(2)}(\kappa|x-x'|)\, dx' \\ I &= 2\, e^{-j\kappa x \sin\theta}. \end{aligned}\right\} \quad x\varepsilon S \tag{10}$$

Since [5, Appendix D]

$$H_0^{(2)}(\xi) = J_0(\xi) - jN_0(\xi) \tag{11}$$

where J_0 and N_0 are the Bessel functions of the first kind and zero order and of the second kind and zero order, respectively, Y(M) can be written as

$$Y(M) = G(M) + jB(M) \tag{12}$$

where

$$\left.\begin{aligned} G(M) &= \frac{\kappa}{\zeta} \int_{-w}^{w} M(x')\, J_0(\kappa|x-x'|)\, dx' \\ B(M) &= -\frac{\kappa}{\zeta} \int_{-w}^{w} M(x')\, N_0(\kappa|x-x'|)\, dx'. \end{aligned}\right\} \quad x\varepsilon S \tag{13}$$

Following Harrington and Mautz [2], the characteristic currents of the slot are defined to be the eigenfunctions M_n of the eigenvalue operator equation

$$Y(M_n) = y_n\, G(M_n) \tag{14}$$

and are so normalized that

$$\langle M_n,\, G(M_n)\rangle = 1. \tag{15}$$

In (15), $\langle .,. \rangle$ denotes the inner product

$$\langle C,\, D\rangle = \int_{-w}^{w} C^*(x)\, D(x)\, dx \tag{16}$$

where $C^*(x)$ is the complex conjugate of $C(x)$. Put

$$y_n = 1 + jb_n. \tag{17}$$

Then, using (12) and (17), (14) becomes

$$B(M_n) = b_n\, G(M_n). \tag{18}$$

Clearly, Y is symmetric (with respect to primed and unprimed coordinates), and so are G and B. G and B are also self-adjoint, since for any M_1 and M_2

$$\begin{aligned} \langle M_1,\, G(M_2)\rangle &= \langle M_1,\, \tfrac{1}{2}\,(Y + Y^*)(M_2)\rangle \\ &= \langle \tfrac{1}{2}\,(Y + Y^*)(M_1),\, M_2\rangle \\ &= \langle G(M_1),\, M_2\rangle \end{aligned} \tag{19}$$

and similarly for B. Furthermore, G is positive definite, since the time-average power radiated into the $z>0$ half-space

$$P_{rad} = \frac{1}{2}\,\mathrm{Re}\left\{\int_{-w}^{w} \underline{E} \times \underline{H}^{*}\Big|_{z=0_+} \cdot \underline{z}\, dx\right\}$$

$$= \frac{1}{2}\,\mathrm{Re}\left\{\frac{1}{2}\langle Y(M),\, M\rangle\right\}$$

$$= \frac{1}{4}\langle G(M),\, M\rangle \tag{20}$$

is always positive. The second equality in (20) follows from (4), (5), (6), (7), and (10). It is then a standard practice [6, Section 1-25] to prove that all b_n, and hence M_n, are real, and that M_n can be chosen to satisfy the orthogonality relationships

$$\left.\begin{aligned} &1.\ \langle M_m,\, G(M_n)\rangle = \delta_{nm} \\ &2.\ \langle M_m,\, B(M_n)\rangle = b_n\,\delta_{nm} \\ &3.\ \langle M_m,\, Y(M_n)\rangle = (1 + jb_n)\,\delta_{nm} \end{aligned}\right\} \tag{21}$$

where δ_{nm} is the Kronecker delta function (0 if $m \neq n$, and 1 if $m=n$).

All the currents on a slot in an infinite screen in an unbounded medium are required to radiate some power however small. As can be seen from (18) and (20), the characteristic currents corresponding to very large b's are basically non-radiating. In the limit as $b \to \infty$, these currents cannot therefore possibly exist. Only when the $z>0$ region is bounded by a perfect conductor, so that no radiation occurs, these currents are physically present. (G is then positive semi-definite rather than positive definite.) When the slot is very narrow, this is almost true, and such currents can be evaluated under narrow slot approximations, as is shown in a later section. In any case, however, all the

currents have to exhibit the edge property $\left(O\left(\frac{1}{\sqrt{w^2-x^2}}\right) \text{ as } x \to \pm w\right)$ [7, Section 1-4].

4. Modal Solution of the Operator Equation

A modal solution of (9) for the magnetic current M over the slot is obtained in this section.

Put

$$M = \sum_n V_n M_n \tag{22}$$

where M_n are the characteristic currents of the slot, and V_n are complex coefficients to be determined. Substituting (22) into (9), there then results

$$\sum_n V_n Y(M_n) = I. \tag{23}$$

Taking the inner product of (23) with each M_m, one obtains

$$\sum_n V_n \langle M_m, Y(M_n)\rangle = \langle M_m, I\rangle. \tag{24}$$

Because of the third orthogonality relationship of (21), only the mth term in the summation survives. Thus

$$V_m = \frac{\langle M_m, I\rangle}{1 + jb_m} \quad . \tag{25}$$

Substituting (25) into (22), M then becomes

$$M = \sum_n \frac{\langle M_n, I\rangle}{1 + jb_n} M_n. \tag{26}$$

The magnetic current M given by (26) is called the modal solution of (9).

5. Power Considerations

The total complex power entering the slot is basically

$$P_{in} = \int_{-w}^{w} \underline{E} \times \underline{H}^* \Big|_{z=0_-} \cdot \underline{z}\, dx. \tag{27}$$

Using (3), (4), (5), (6), (7), (9) and (10), (27) becomes

$$\begin{aligned} P_{in} &= \langle I, M\rangle - \frac{1}{2}\langle Y(M), M\rangle \\ &= \frac{1}{2}\langle I, M\rangle \\ &= \frac{1}{2}\langle Y(M), M\rangle. \end{aligned} \tag{28}$$

Furthermore, using (26), (28) becomes

$$P_{in} = \frac{1}{2}\left\{ \sum_n \frac{1 - jb_n}{1 + b_n^2} |\langle I, M_n\rangle|^2 \right\}. \tag{29}$$

A comparison of (20) and (28) then shows that the complex power transmitted through the slot is also given by (29).

A parameter sometimes used to express the transmission characteristics of the slot is the transmission coefficient T. By definition, the transmission coefficient of the slot is the ratio of the time-

average power transmitted through the slot to that incident on the slot [5, Section 7-12]. Using (1) and (29), T is readily found as

$$T = \frac{1}{4w\zeta \cos\theta} \sum_n \frac{1}{1 + b_n^2} |\langle I, M_n \rangle|^2. \tag{30}$$

6. The Characteristic Fields of the Slot

The fields $(\underline{E}_n, \underline{H}_n)$ produced by the characteristic currents M_n are called the characteristic fields of the slot. Orthogonality relationships for the characteristic fields over the radiation cylinder can be obtained from those for the characteristic currents by means of the complex Poynting theorem [5, Section 1-10]. These relationships are dual to those for the characteristic fields of a conducting body, and can be derived in a similar manner [8]. Thus

$$\left.\begin{aligned}
&1.\ \frac{2}{\zeta} \int_{Cy_\infty} \underline{E}_m^* \cdot \underline{E}_n \, d\tau = \delta_{nm} \\
&2.\ 2\zeta \int_{Cy_\infty} \underline{H}_m^* \cdot \underline{H}_n \, d\tau = \delta_{nm} \\
&3.\ 2\omega \int_V (\mu \underline{H}_m^* \cdot \underline{H}_n - \varepsilon \underline{E}_m^* \cdot \underline{E}_n) \, dv = - b_n \delta_{nm}
\end{aligned}\right\} \tag{31}$$

in duality with those for a conducting body. In (31), Cy_∞ is the radiation cylinder, and the integration in (31.3) is over the whole space. Figure 3 shows the integration domain for (31).

The third orthogonality relationship of (31) states that the difference between the magnetic and electric energy stored in any characteris-

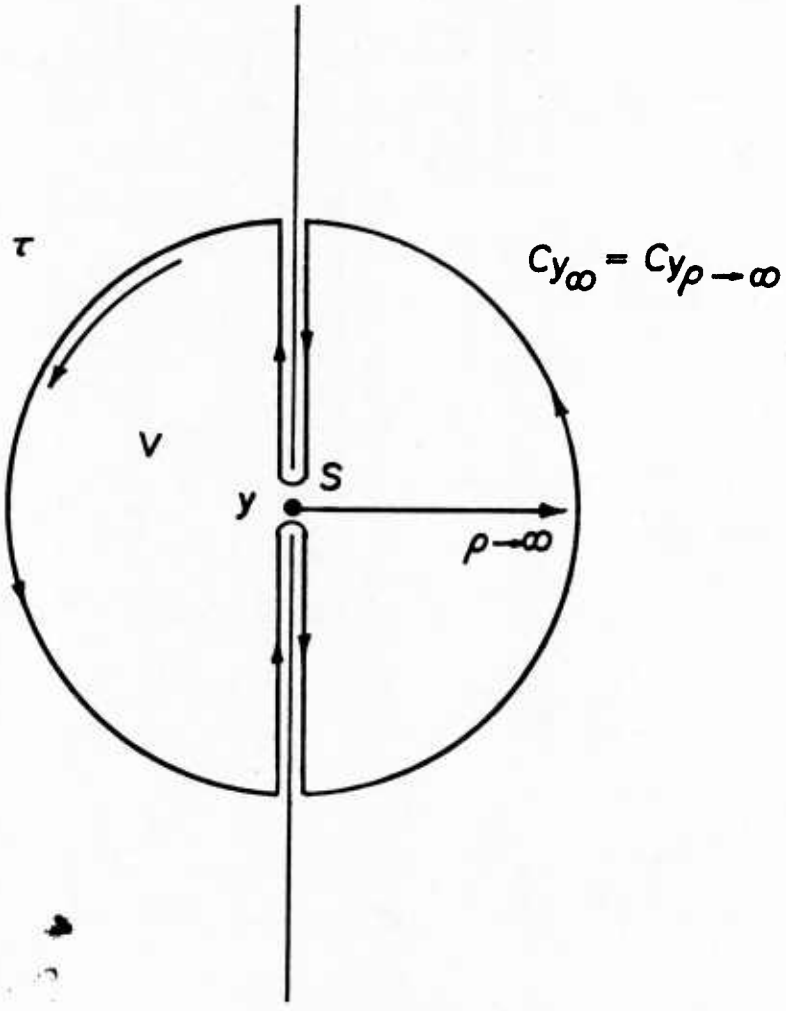

FIG. 3

THE INTEGRATION DOMAIN OF (31)

tic field is $-b/2\omega$ Joules for every one Watt of radiated power. The characteristic fields corresponding to positive (negative) b have predominantly stored electric (magnetic) energy, and are therefore referred to as the capacitive (inductive) modes of the slot. The characteristic fields corresponding to b=0 are called the resonant modes of the slot.

A modal expansion of the field radiated by M in terms of the characteristic fields $\underline{E}_n$ and $\underline{H}_n$ can readily be obtained using the modal expansion (22) of M:

$$\left.\begin{aligned} \underline{E}(\underline{M}) &= \sum_n V_n \underline{E}(\underline{M}_n) = \sum_n V_n \underline{E}_n \\ \underline{H}(\underline{M}) &= \sum_n V_n \underline{H}(\underline{M}_n) = \sum_n V_n \underline{H}_n . \end{aligned}\right\} \tag{32}$$

In the Appendix, it is shown that the field $(\underline{E}(\underline{M}), \underline{H}(\underline{M}))$ given by (32) converges in a least squares sense on the radiation cylinder.

7. The Narrow Slot

An important case that requires a special consideration is that of the narrow slot ($2w\kappa << 1$).

Since

$$\kappa|x-x'| \leq 2w\kappa << 1 \tag{33}$$

the Bessel functions J_0 and N_0 can be replaced by their small argument approximations [5, Appendix D]:

$$\left.\begin{aligned} J_0(\kappa|x-x'|) &\simeq 1 - \frac{\kappa^2}{4}|x-x'|^2 \\ N_0(\kappa|x-x'|) &\simeq \frac{2}{\pi}\log\left(\frac{\gamma\kappa}{2}|x-x'|\right) \end{aligned}\right\} \tag{34}$$

where log denotes the natural logarithm, and γ=1.7810724. G(M) and B(M) are then given by

$$\left.\begin{aligned} G(M) &\simeq \frac{\kappa}{\zeta}\int_{-w}^{w} M(x')\left\{1 - \frac{\kappa^2}{4}|x-x'|^2\right\} dx' \\ B(M) &\simeq -\frac{2\kappa}{\pi\zeta}\int_{-w}^{w} M(x')\log\left\{\frac{\gamma\kappa}{2}|x-x'|\right\} dx' \end{aligned}\right\} \quad x\varepsilon S \tag{35}$$

Furthermore, I does not vary appreciably over S, and can therefore be approximated by the first two terms of its Taylor expansion about x=0. That is

$$I \simeq 2 - j2\kappa\, x\, \sin\theta, \qquad x\varepsilon S. \tag{36}$$

Using (3), I then becomes

$$I \simeq H_y^{sc}(0) + j\frac{\kappa}{\zeta}\, E_z^{sc}(0)\, x, \qquad x\varepsilon S \tag{37}$$

where (0) is written for the point (x,z)=(0,0).

The characteristic currents of the narrow slot can be determined by solving (18) with G(M) and B(M) given by (35), viz.:

$$-\frac{2}{\pi}\int_{-w}^{w} M_n(x')\,\log\left\{\frac{\gamma\kappa}{2}|x-x'|\right\}\,dx'$$

$$= b_n \int_{-w}^{w} M_n(x')\left\{1-\frac{\kappa^2}{4}|x-x'|^2\right\}\,dx', \qquad x\varepsilon S \tag{38}$$

An exact solution of (38) is possible: Using the identities

$$\left.\begin{aligned}
&\int_{-w}^{w}\frac{1}{\sqrt{w^2-x'^2}}\,dx' = \pi\\
&\int_{-w}^{w}\frac{1}{\sqrt{w^2-x'^2}}\,\log\left\{\frac{\gamma\kappa}{2}|x-x'|\right\}\,dx' = \pi\,\log\left\{\frac{\gamma\kappa w}{4}\right\}
\end{aligned}\right\} \tag{39}$$

it readily follows that

$$\left.\begin{aligned}
M_1 &= \frac{U_1}{\sqrt{w^2-x^2}}\\
b_1 &= -\frac{2}{\pi}\,\log\left\{\frac{\gamma\kappa w}{4}\right\}
\end{aligned}\right\} \tag{40}$$

is a solution pair of (38). Similarly, it follows from the identities

$$\left.\begin{aligned}
&\int_{-w}^{w}\frac{x'^2}{\sqrt{w^2-x'^2}}\,dx' = \frac{w^2\pi}{2}\\
&\int_{-w}^{w}\frac{x'}{\sqrt{w^2-x'^2}}\,\log\left\{\frac{\gamma\kappa}{2}|x-x'|\right\}\,dx' = -\pi\,x
\end{aligned}\right\} \tag{41}$$

that

$$\left.\begin{aligned} M_2 &= \frac{U_2 x}{\sqrt{w^2-x^2}} \\ b_2 &= \frac{8}{\pi \kappa^2 w^2} \end{aligned}\right\} \tag{42}$$

is another solution pair of (38). In fact, these solution pairs are the only possible solutions to (38), as can readily be verified from the identity [9, Appendix]

$$\int_{-w}^{w} \frac{T_n(\frac{x'}{w})}{\sqrt{w^2-x'^2}} \log\left(|x-x'|\right) dx' = \begin{cases} -\pi \log(\frac{2}{w})\, T_0(\frac{x}{w}) & \text{if } n=0 \\ -\frac{\pi}{n} T_n(\frac{x}{w}) & \text{if } n>0 \end{cases} \tag{43}$$

where T_n is the Chebyshev polynomial of the first kind and nth order, and the two identities in (39) and (41) involving logarithms are the n=0 and n=1 cases of (43), respectively. In (40) and (42), U_1 and U_2 are constants to be determined according to (15). Thus

$$M_1 = \frac{1}{\pi}\sqrt{\frac{\zeta}{\kappa}}\,\frac{1}{\sqrt{w^2-x^2}} \tag{44}$$

$$M_2 = \frac{2}{\pi \kappa w^2}\sqrt{\frac{2\zeta}{\kappa}}\,\frac{x}{\sqrt{w^2-x^2}}\,. \tag{45}$$

Furthermore, it readily follows from (40) and (42) that the charcteristic values of the narrow slot are very large positive numbers whose ratio satisfies

$$\frac{b_2}{b_1} = \frac{-4}{\log\left(\frac{\gamma\kappa w}{4}\right)\kappa^2 w^2} \geq \frac{4}{(1-\frac{\gamma\kappa w}{4})\,\kappa^2 w^2} \simeq \left[\frac{2}{\kappa w}\right]^2. \tag{46}$$

The equivalent magnetic current M of the narrow slot is now given by

$$M = \frac{\langle M_1, I\rangle}{1 + jb_1} M_1 + \frac{\langle M_2, I\rangle}{1 + jb_2} M_2$$

$$\simeq \frac{\langle M_1, I\rangle}{1 + jb_1} M_1 - j \frac{\langle M_2, I\rangle}{b_2} M_2$$

$$= \frac{1}{2} \left\{ j\frac{\zeta}{\kappa} \frac{H_y^{sc}(0)}{\nu + \log\left(\frac{\kappa w}{4}\right) + j\frac{\pi}{2}} + E_z^{sc}(0)\, x \right\} \frac{1}{\sqrt{w^2 - x^2}} \tag{47}$$

as readily follows by substituting (37), (40), (42), (44) and (45) into (26). In (47), $\nu = \log(\gamma)$ is the Euler's constant. Higher order solutions can be obtained by retaining more terms in the small argument approximations of Bessel functions in (34), but, in view of (46), the contribution of the higher order characteristic currents is negligible. Incidentally, the magnetic current in (47) is identical with the solution given in [9].

8. Solution of the Eigenvalue Equation

An exact solution of the eigenvalue equation (18) for the characteristic currents is rather difficult, if at all possible. An approximate solution has then to be sought.

Put

$$S = \bigcup_{k=1}^{N} S_k \tag{48}$$

$$M_n \simeq \sum_{k=1}^{N} U_{nk} P_k. \tag{49}$$

In (48), S_k are non-overlapping intervals such that

$$2w = \sum_{k=1}^{N} |S_k| \tag{50}$$

where $|S_k|$ is the length of the kth interval (see Figure 4). In (49), each P_k is a real function, yet to be specified, that vanishes on $S_{\ell \neq k}$, and U_{nk} are real coefficients to be determined. Substituting (49) into (18), it becomes

$$\sum_{k=1}^{N} U_{nk} B(P_k) = b_n \sum_{k=1}^{N} U_{nk} G(P_k) + R \tag{51}$$

where R is a residual term.

A Galerkin solution [10, Section 1-3] of (18) can be obtained by requiring that R be orthogonal to all P_ℓ, viz.:

$$\langle P_\ell, R \rangle = 0, \qquad \ell = 1,2,..,N. \tag{52}$$

Thus, taking the inner product of (51) with each P_ℓ, and enforcing the Galerkin condition (52), there then results

$$\sum_{k=1}^{N} U_{nk} \langle P_\ell, B(P_k) \rangle = b_n \sum_{k=1}^{N} U_{nk} \langle P_\ell, G(P_k) \rangle, \quad \ell=1,2,..,N. \tag{53}$$

In matrix form, (53) becomes

$$\overline{\overline{B}}\, \vec{U}_n = b_n \overline{\overline{G}}\, \vec{U}_n \tag{54}$$

where $\overline{\overline{G}}$ and $\overline{\overline{B}}$ are the N by N matrices

$$\left.\begin{aligned} \overline{\overline{G}} &= [G_{\ell k}] = [\langle P_\ell, G(P_k) \rangle] \\ \overline{\overline{B}} &= [B_{\ell k}] = [\langle P_\ell, B(P_k) \rangle] \end{aligned}\right\} \tag{55}$$

and $\vec{U}_n$ is the N by 1 vector

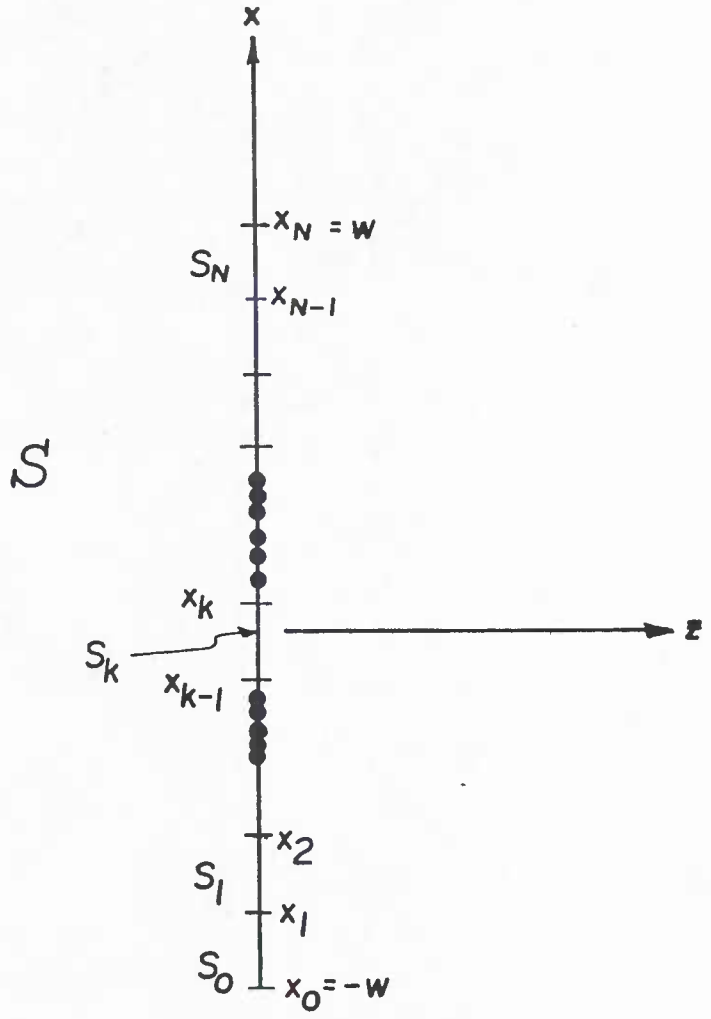

FIG. 4

THE PARTITION OF THE SLOT

$$\vec{U}_n = [U_{nk}]. \tag{56}$$

The constraint equation (15) now becomes

$$\vec{U}_n^T \bar{\bar{G}} \vec{U}_n = 1 \tag{57}$$

where the superscript T denotes vector transpose.

The solution of (54) subject to (57) determines in a Galerkin sense the first N characteristic currents of the slot.

9. Evaluation of the Matrices $\bar{\bar{G}}$ and $\bar{\bar{B}}$

The evaluation of the matrices $\bar{\bar{G}}$ and $\bar{\bar{B}}$ constitutes a large portion of the work involved in the solution. An efficient evaluation of these matrices is therefore necessary for the success of the solution.

The ℓkth elements of $\bar{\bar{G}}$ and $\bar{\bar{B}}$ are given by

$$\left.\begin{aligned} G_{\ell k} &= \int_{x_{\ell-1}}^{x_\ell} P_\ell(x)\,dx \int_{x_{k-1}}^{x_k} P_k(x')\, J_0(\kappa|x-x'|)\,dx' \\ B_{\ell k} &= -\int_{x_{\ell-1}}^{x_\ell} P_\ell(x)\,dx \int_{x_{k-1}}^{x_k} P_k(x')\, N_0(\kappa|x-x'|)\,dx' \end{aligned}\right\} \tag{58}$$

where P_k are so far unspecified. A particularly simple choice for P_k is

$$P_k = \begin{cases} 1 & \text{on } S_k \\ 0 & \text{on } S_{\ell \neq k} \end{cases} \tag{59}$$

which corresponds to a pulse expansion of the characteristic currents. Using (59), the ℓkth elements of $\bar{\bar{G}}$ and $\bar{\bar{B}}$ become

$$\left.\begin{aligned} G_{\ell k} &= \int_{x_{\ell-1}}^{x_\ell} dx \int_{x_{k-1}}^{x_k} J_0(\kappa|x-x'|)\, dx' \\ B_{\ell k} &= -\int_{x_{\ell-1}}^{x_\ell} dx \int_{x_{k-1}}^{x_k} N_0(\kappa|x-x'|)\, dx'. \end{aligned}\right\} \tag{60}$$

Put

$$\left.\begin{aligned} \hat{G}_{\ell k}(x) &= \int_{x_{k-1}}^{x_k} J_0(\kappa|x-x'|)\, dx' \\ \hat{B}_{\ell k}(x) &= -\int_{x_{k-1}}^{x_k} N_0(\kappa|x-x'|)\, dx' \end{aligned}\right\} \quad x\varepsilon S_\ell. \tag{61}$$

Then, by the first mean value theorem for integration [11, Section 7-18] there exists points x_{J_0}, $x_{N_0} \varepsilon S_\ell$ such that

$$\left.\begin{aligned} G_{\ell k} &= |S_\ell|\, \hat{G}_{\ell k}(x_{J_0}) \\ B_{\ell k} &= |S_\ell|\, \hat{B}_{\ell k}(x_{N_0}). \end{aligned}\right\} \tag{62}$$

The evaluation of $G_{\ell k}$ and $B_{\ell k}$ is completed by integrating the Bessel functions J_0 and N_0 over S_k, and, for that purpose, any quadrature rule can be used. Thus

$$\left.\begin{aligned} G_{\ell k} &\simeq \frac{1}{2}\,|S_\ell||S_k| \sum_{i=1}^{Q} q_i\, J_0\left(\kappa\left|x_{J_0} - \left(x_{k+\frac{1}{2}} + p_i\,\frac{|S_k|}{2}\right)\right|\right) \\ B_{\ell k} &\simeq -\frac{1}{2}\,|S_\ell||S_k| \sum_{i=1}^{Q} q_i\, N_0\left(\kappa\left|x_{N_0} - \left(x_{k+\frac{1}{2}} + p_i\,\frac{|S_k|}{2}\right)\right|\right). \end{aligned}\right\} \tag{63}$$

In (63), Q is the order of the rule, q_i are its coefficients, p_i determine the location of its abscissas, and

$$x_{k+\frac{1}{2}} = (x_{k+1} + x_k) \div 2 \tag{64}$$

is the midpoint of S_k.

When evaluating the diagonal elements of $\overline{\overline{B}}$ ($\ell=k$), N_0 offers a logarithmic singularity at $x=x'$ that requires particular attention. Put

$$N_{0p}(\kappa|x-x'|) = (N_0 - N_{0s})(\kappa|x-x'|) \tag{65}$$

where N_{0s} is the singular part of N_0 given by its small argument approximation (34). Then

$$\begin{aligned} B_{\ell\ell} &= -\int_{x_{\ell-1}}^{x_\ell} dx \int_{x_{\ell-1}}^{x_\ell} (N_{0s} + N_{0p})(\kappa|x-x'|)\, dx' \\ &= -\frac{1}{\pi}\,|S_\ell|^2 \left[2\,\log\left(\gamma\kappa\,\frac{|S_\ell|}{2}\right) - 3\right] - \int_{x_{\ell-1}}^{x_\ell} dx \int_{x_{\ell-1}}^{x_\ell} N_{0p}(\kappa|x-x'|)\, dx'. \end{aligned} \tag{66}$$

N_{0p} has no singularity at $x=x'$, and can therefore be integrated by the first mean value theorem and quadratures. Thus

$$B_{\ell\ell} \simeq -\frac{1}{\pi}|S_\ell|^2\left[2\log\left(\gamma\kappa\frac{|S_\ell|}{2}\right)-3\right]$$

$$-\frac{1}{2}|S_\ell|^2\sum_{i=1}^{Q} q_i N_{0p}\left(\kappa\left|x_{N_{0p}}-\left(x_{\ell+\frac{1}{2}}+p_i\frac{|S_\ell|}{2}\right)\right|\right) \qquad (67)$$

for some $x_{N_{0p}} \varepsilon S_\ell$.

Actually, finding such points x_{J_0}, x_{N_0}, and $x_{N_{0p}}$ is at least as difficult as computing the integrals themselves. For sufficiently small $|S_\ell|$, however, the midpoint of S_ℓ can replace these points while introducing nearly no error. Thus, eliminating the common factor $|S_\ell|$,

$$G_{\ell k} \simeq \frac{1}{2}|S_k|\sum_{i=1}^{Q} q_i J_0(u_i^{\ell k}) \qquad \text{for all } \ell,k$$

$$B_{\ell k} \simeq \begin{cases} -\frac{1}{2}|S_k|\sum_{i=1}^{Q} q_i N_0(u_i^{\ell k}) & \text{if } \ell\neq k \\ -|S_\ell|\left\{\frac{1}{\pi}\left[2\log\left(\gamma\kappa\frac{|S_\ell|}{2}\right)-3\right]+\frac{1}{2}\sum_{i=1}^{Q} q_i N_{0p}(u_i^{\ell k})\right\} & \text{if } \ell=k \end{cases} \qquad (68)$$

where

$$u_i^{\ell k} = \kappa\left|x_{\ell+\frac{1}{2}}-\left(x_{k+\frac{1}{2}}+p_i\frac{|S_k|}{2}\right)\right|. \qquad (69)$$

The matrices $\bar{\bar{G}}$ and $\bar{\bar{B}}$ so obtained are the same as those would result from enforcing the point matching condition

$$R(x_{\ell+\frac{1}{2}}) = 0, \qquad \ell=1,2,..,N \qquad (70)$$

in (51) rather than the Galerkin condition (52), except for a slight alteration in $B_{\ell\ell}$, as can easily be established.

10. Numerical Results

The characteristic currents and fields, as well as the equivalent magnetic current, radiation pattern, and transmission coefficient, have been computed for different slot widths. Some of the results obtained for the 0.4λ, 0.5λ, and 1.0λ slots are given in this section.

In the actual computation, polynomial expansions of the Bessel functions J_0 and N_0 [12, Articles 9-4.1,2,3] are utilized, while all the integrals are computed using an eight-point Gaussian quadrature [12, Table 25.4]. In evaluating the far fields, the Hankel function is first replaced by its large argument approximation [5, Appendix D]:

$$H_0^{(2)}(\xi) \simeq \sqrt{\frac{2j}{\pi\xi}}\, e^{-j\xi}. \tag{71}$$

Then, using the typical radiation zone approximations [5, Section 2-10],

$$\left.\begin{aligned} \xi &= \kappa\sqrt{z^2 + (x-x')^2} \simeq \kappa(\rho - x'\cos\psi) \\ \frac{1}{\xi} &\simeq \frac{1}{\kappa\rho} \end{aligned}\right\} \tag{72}$$

for all points $(x,z)\varepsilon Cy_\rho$, $\rho>>2w$, where ψ is the angle $\underline{\rho}=x\underline{x}+z\underline{z}$ makes with the x-axis, the electric vector potential produced by the characteristic current M_n at any point $(\rho,\psi)\varepsilon Cy_\rho$ is readily found as

$$\underline{F}(\underline{M}_n) \simeq \left\{ \frac{1}{\sqrt{2j\pi\kappa\rho}} e^{-j\kappa\rho} \sum_{k=1}^{N} U_{nk} \int_{x_k}^{x_{k+1}} e^{j\kappa x' \cos\psi} \, dx' \right\} \underline{y}$$

$$\simeq \left\{ A(\kappa\rho) \sum_{k=1}^{N} U_{nk} |S_k| \, e^{j\kappa x_{k+\frac{1}{2}} \cos\psi} \right\} \underline{y}. \qquad (73)$$

The far characteristic fields then follow by substituting (73) into (6).

An IMSL Library 2 subroutine "EIGZF" [13] is used to solve the matrix eigenvalue equation (54) for the characteristic values and currents In all the computer runs, a "performance index" has consistently come less than one, indicating that the subroutine has performed well. The convergence patterns for the characteristic values for the 0.4λ, 0.5λ, and 1.0λ slots are shown in Tables 1, 2, and 3, respectively. As can be seen, the convergence is always montone, either upwardly, or downwardly. Only for the 1.0λ slot, b_2 first decreases monotonically, but later increases, although this can be attributed to rounding errors. Furthermore, the convergence of the lower order characteristic values is generally faster than that of the higher order ones. The convergence of the dominant characteristic current for these slots is shown in Figures 5, 11, and 17.

The last columns in Tables 1, 2, and 3 warrant an explanation. "EIGZF" returns pairs of numbers whose quotients determine the characteristic values. Both numbers are checked, and when the divisor of any such pair is found to be an exact zero, an infinte value is assigned to the characteristic value. Furthermore, the power radiated by the corresponding characteristic current has always been found to be exactly zero. Unfortunately, it is not true that only a finite number of char-

Table 1. The convergence of the characteristic values for a 0.4λ slot.

N	b_1	b_2	b_3	b_4	b_5	...
4	0.3864999	2.5419659	52.9851044	7.2047462×10^{3}	*	*
8	0.3829608	2.3814417	39.5235940	2.7784331×10^{3}	4.6240706×10^{5}	∞
12	0.3819787	2.3403592	37.0742823	2.3726822×10^{3}	3.3298869×10^{5}	∞
16	0.3815764	2.3221121	36.0919691	2.2324162×10^{3}	2.9452827×10^{5}	∞
20	0.3813810	2.3119735	35.5731692	2.1634724×10^{3}	2.7752366×10^{5}	∞
→24	0.3812775	2.3055932	35.2564286	2.1232330×10^{3}	2.7000217×10^{5}	∞

Table 2. The convergence of the characteristic values for a 0.5λ slot.

N	b_1	b_2	b_3	b_4	b_5	...
4	0.2486212	1.7228569	22.1775861	1.8489054×10^{3}	*	*
8	0.2514326	1.6158270	16.8422341	0.7267531×10^{3}	0.7674664×10^{5}	∞
12	0.2524255	1.5885171	15.8617172	0.6228877×10^{3}	0.5547073×10^{5}	∞
16	0.2529714	1.5763806	15.4663358	0.5868004×10^{3}	0.4937043×10^{5}	∞
20	0.2533296	1.5696359	15.2567972	0.5690416×10^{3}	0.4661994×10^{5}	∞
→24	0.2535877	1.5653913	15.1285194	0.5586531×10^{3}	0.4505765×10^{5}	∞

Table 3. The convergence of the characteristic values for a 1.0 slot.

N	b_1	b_2	b_3	b_4	b_5	b_6	b_7	...
4	-0.0592173	0.3201691	1.9221747	25.7259409	*	*	*	*
8	-0.0194068	0.3058703	1.6039377	12.3455109	0.2868804×10^{3}	1.4943577×10^{4}	17.0626604×10^{5}	∞
12	-0.0058205	0.3040117	1.5428879	10.9870705	0.2161946×10^{3}	0.8410060×10^{4}	5.5500121×10^{5}	∞
16	0.0009632	0.3034440	1.5176536	10.4968898	0.1953714×10^{3}	0.6970954×10^{4}	4.0148647×10^{5}	∞
20	0.0050257	0.3032162	1.5040598	10.2497418	0.1857875×10^{3}	0.6377427×10^{4}	3.4619262×10^{5}	∞
24	0.0077305	0.3031168	1.4956417	10.1026733	0.1803898×10^{3}	0.6061940×10^{4}	3.1878485×10^{5}	∞
28	0.0096609	0.3030754	1.4899555	10.0059495	0.1769714×10^{3}	0.5870056×10^{4}	3.0428758×10^{5}	∞
32	0.0111081	0.3030634	1.4858791	9.9379017	0.1746300×10^{3}	0.5742663×10^{4}	2.9314329×10^{5}	∞
36	0.0122334	0.3030671	1.4828270	9.8876526	0.1729390×10^{3}	0.5651750×10^{4}	2.8856119×10^{5}	∞
→40	0.0131335	0.3030794	1.4804643	9.8491539	0.1716661×10^{3}	0.5586517×10^{4}	2.8273049×10^{5}	∞

acteristic currents can exist on the slot. Since single precision arithmetic is the mode of operation used in all computations, these characteristic values are actually $O(1/\delta)$, where δ is the smallest positive real number different from zero on the computer. Nevertheless, the contribution of these currents is extremely small, and therefore have not been considered in subsequent computations. It appears that for a slot in a ground plane in an unbounded medium, only a finite number of characteristic currents need to be computed. This is also expected to carry through to slots in a screen separating contrasting mediums.

The computed characteristic currents normalized to a maximum amplitude of unity and their radiation patterns for the slots considered are shown in Figures 6, 8, 12, 14, 18, and 20. This normalization is only for plotting convenience. The equivalent magnetic currents and radiation patterns for the slots are shown in Figures 7, 9, 13, 15, 19, and 21, for the case of normal incidence. It is interesting to note that the number of lobes in each pattern is equal to the order of the characteristic current or field. Finally, Table 4 gives the ratios of the powers radiated by the characteristic currents to that radiated by the dominant characteristic current for each slot, whereas the transmission coefficient for the slots for the case of normal incidence are given in Table 5, all is evaluated with N as specified in the arrow marked rows in Tables 1, 2, and 3. The entries in Table 4 suggest that the radiation pattern for the slot is basically the same as that for its dominant characteristic current. This is indeed the case, as Figures 10, 16, and 22 readily show.

Table 4. The ratio of the power radiated by each characteristic current to that radiated by the dominant characteristic current for a (a) 0.4λ slot, (b) 0.5λ slot, and (c) 1.0λ slot.

(a)

n	P_n / P_1
1	1.0
2	0.1595670
3	5.1706787×10^{-3}
4	6.8070769×10^{-5}
5	5.3741932×10^{-7}
...	0.0

(b)

n	P_n / P_1
1	1.0
2	0.2678140
3	1.1451906×10^{-2}
4	2.3665750×10^{-4}
5	2.9297482×10^{-6}
...	0.0

(c)

n	P_n / P_1
1	1.0
2	0.1496020
3	0.0390829
4	3.7669604×10^{-3}
5	1.7264361×10^{-4}
6	5.2402006×10^{-6}
7	1.1263396×10^{-7}
...	0.0

Table 5. The transmission coeffiecient for the 0.4λ, 0.5λ, and 1.0λ slots for normal incidence.

2w	T
0.4λ	0.9757939
0.5λ	0.9777421
1.0λ	0.9994257

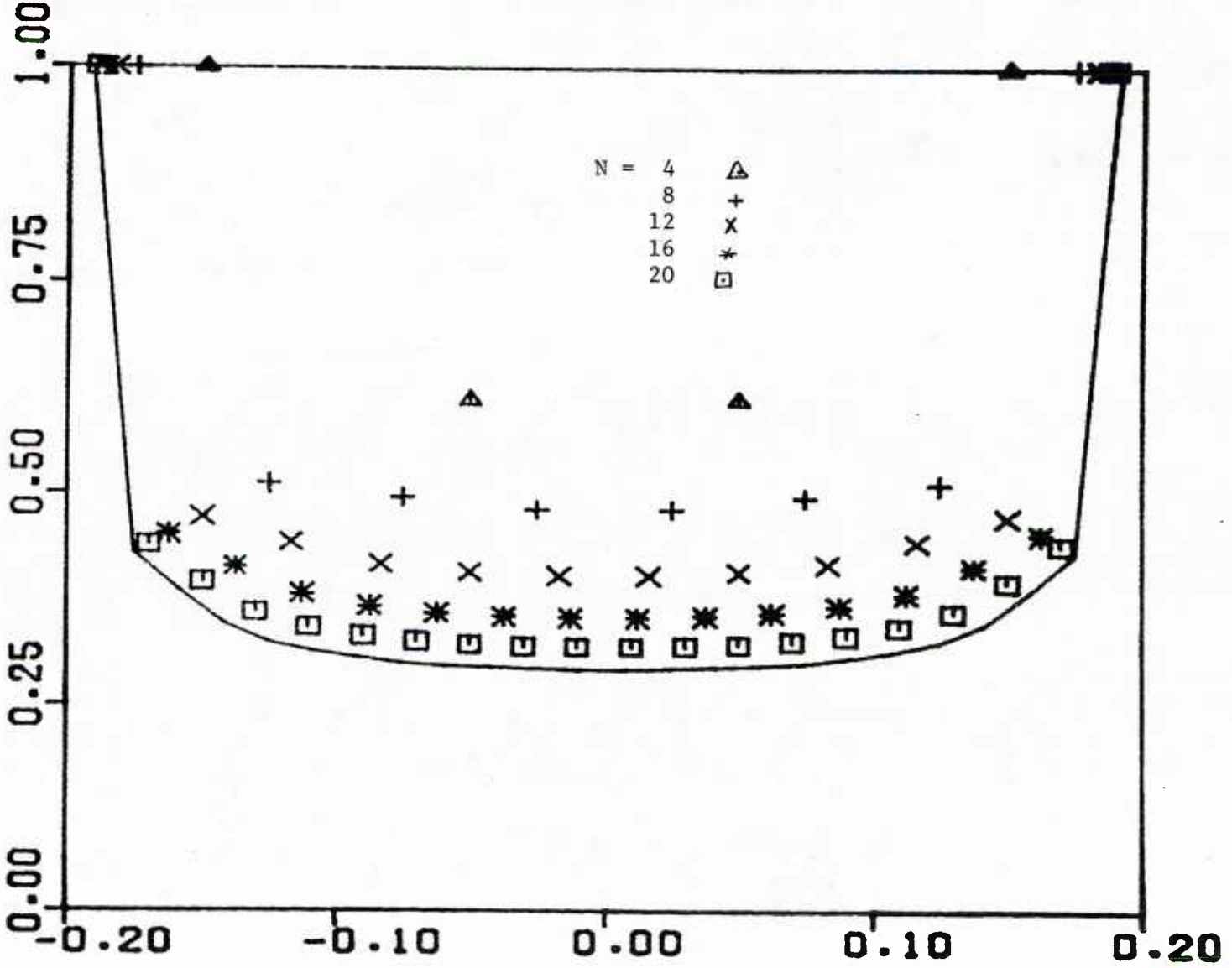

$I_1(x)$

Figure 5: The convergence of the dominant chracteristic current for a 0.4λ slot normalized for a maximum amplitude of unity.

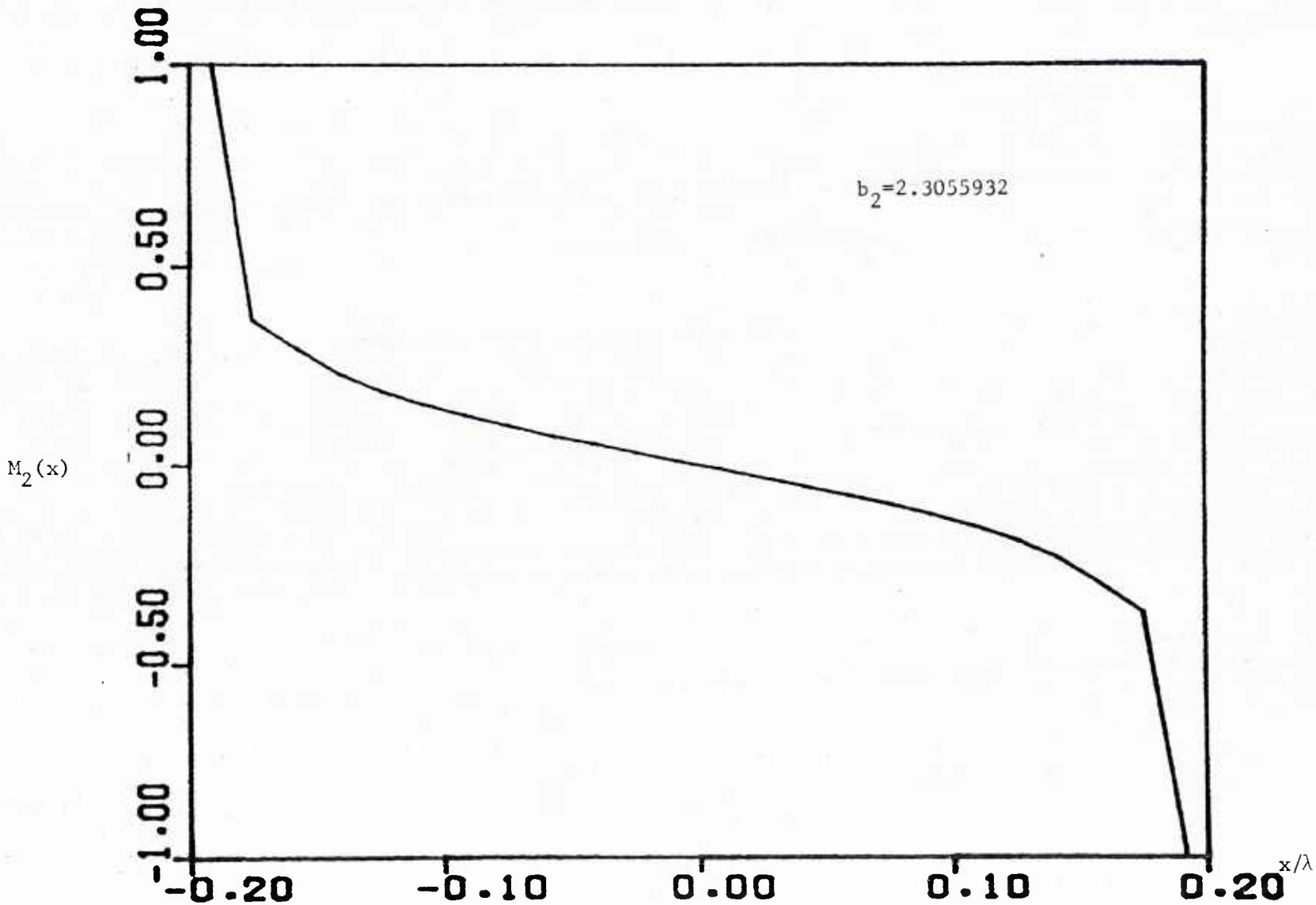

Figure 6. (a) The second,..., (d) fifth characteristic currents for a 0.4 λ slot normalized for a maximum amplitude of unity.

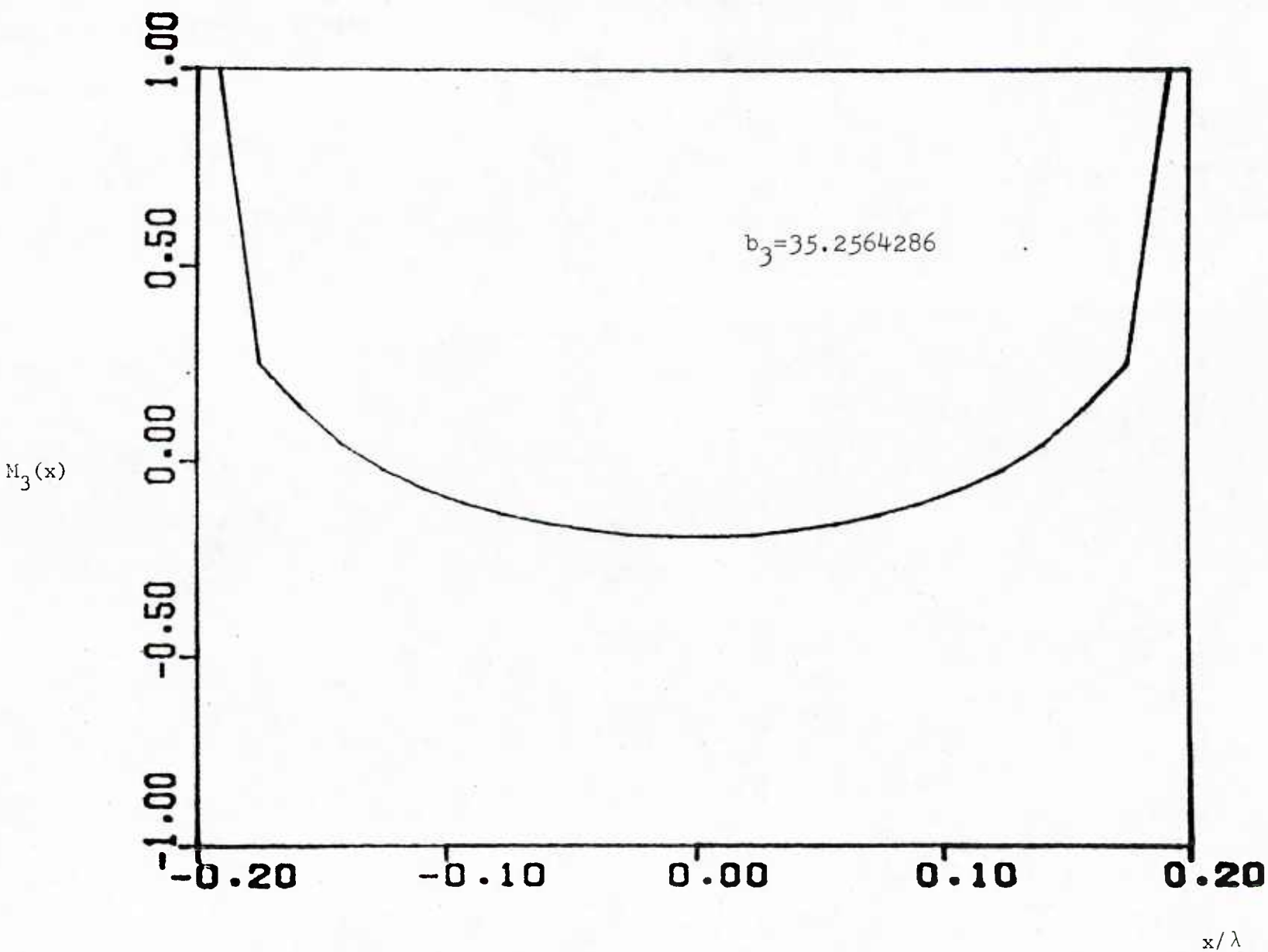

(b)

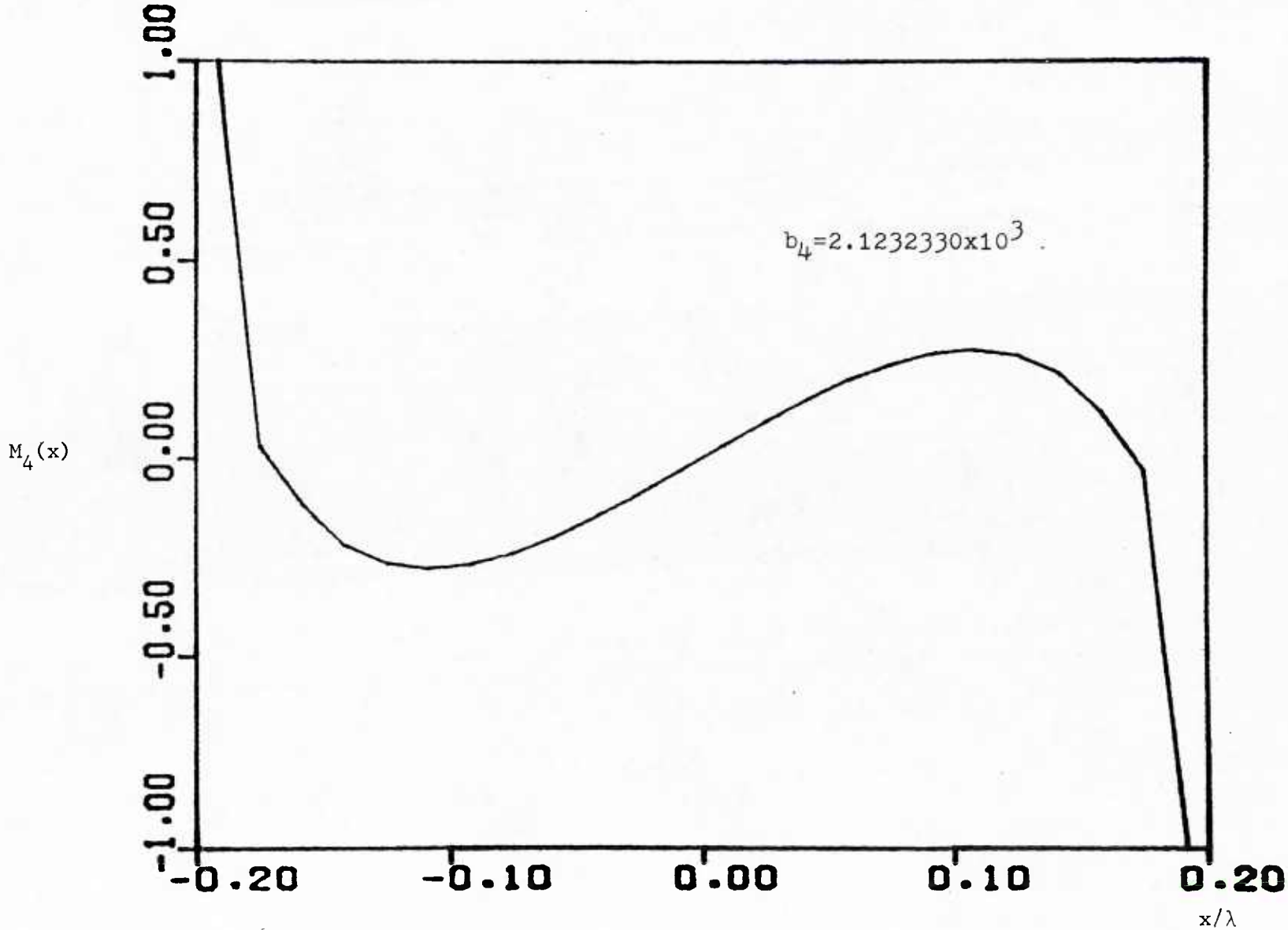

(c)

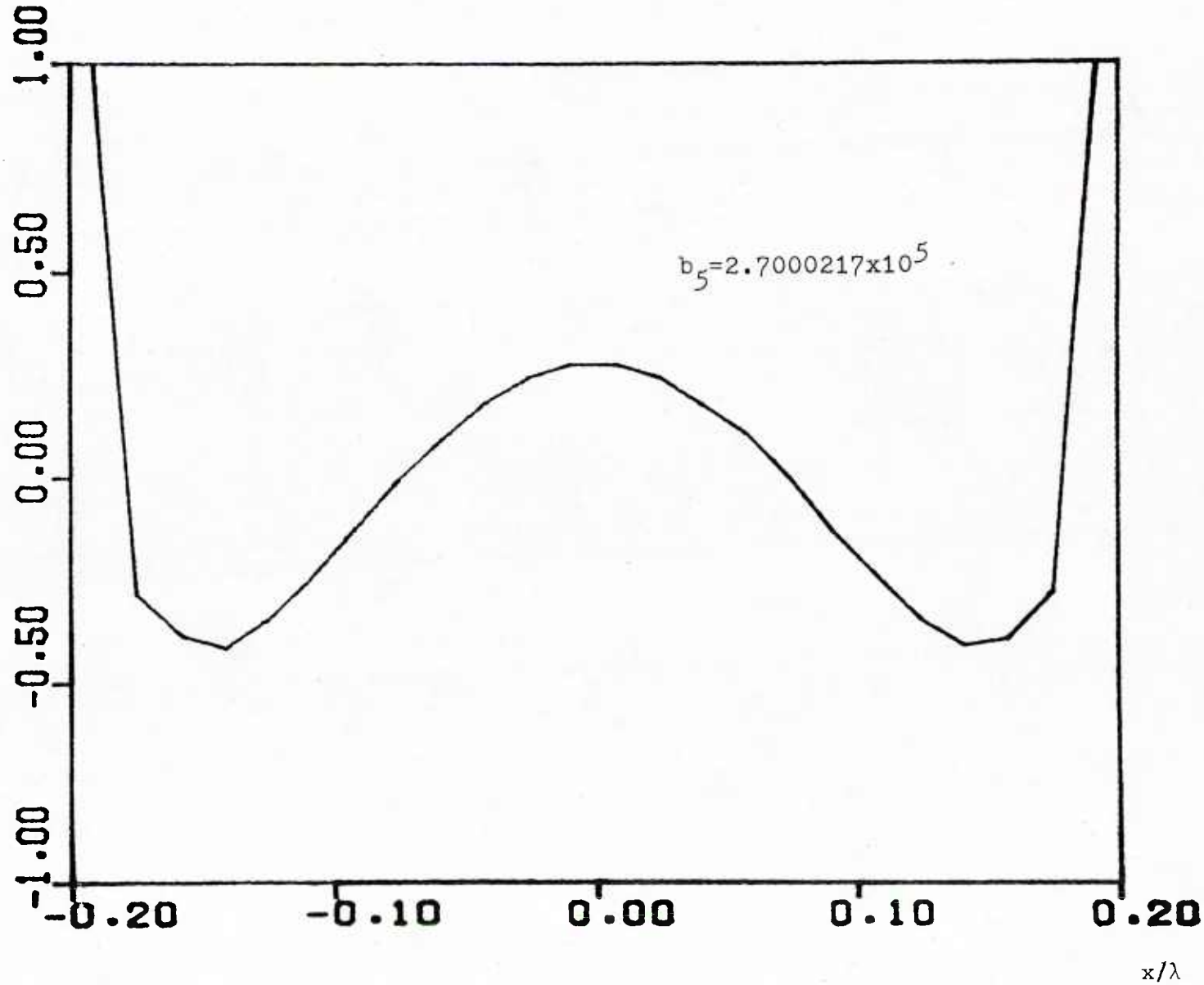

(d)

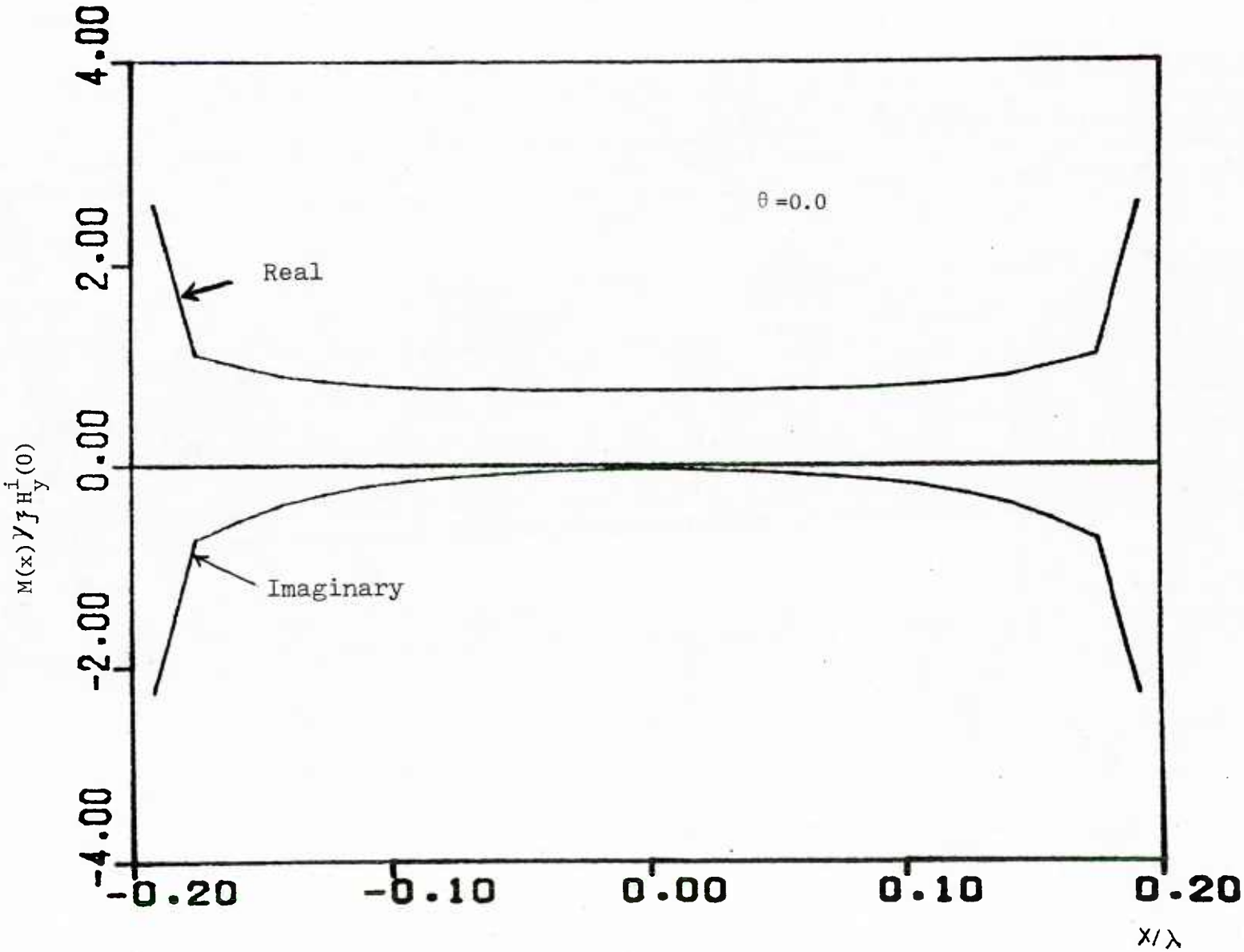

Figure 7: The equivalent magnetic current for a 0.4λ slot.

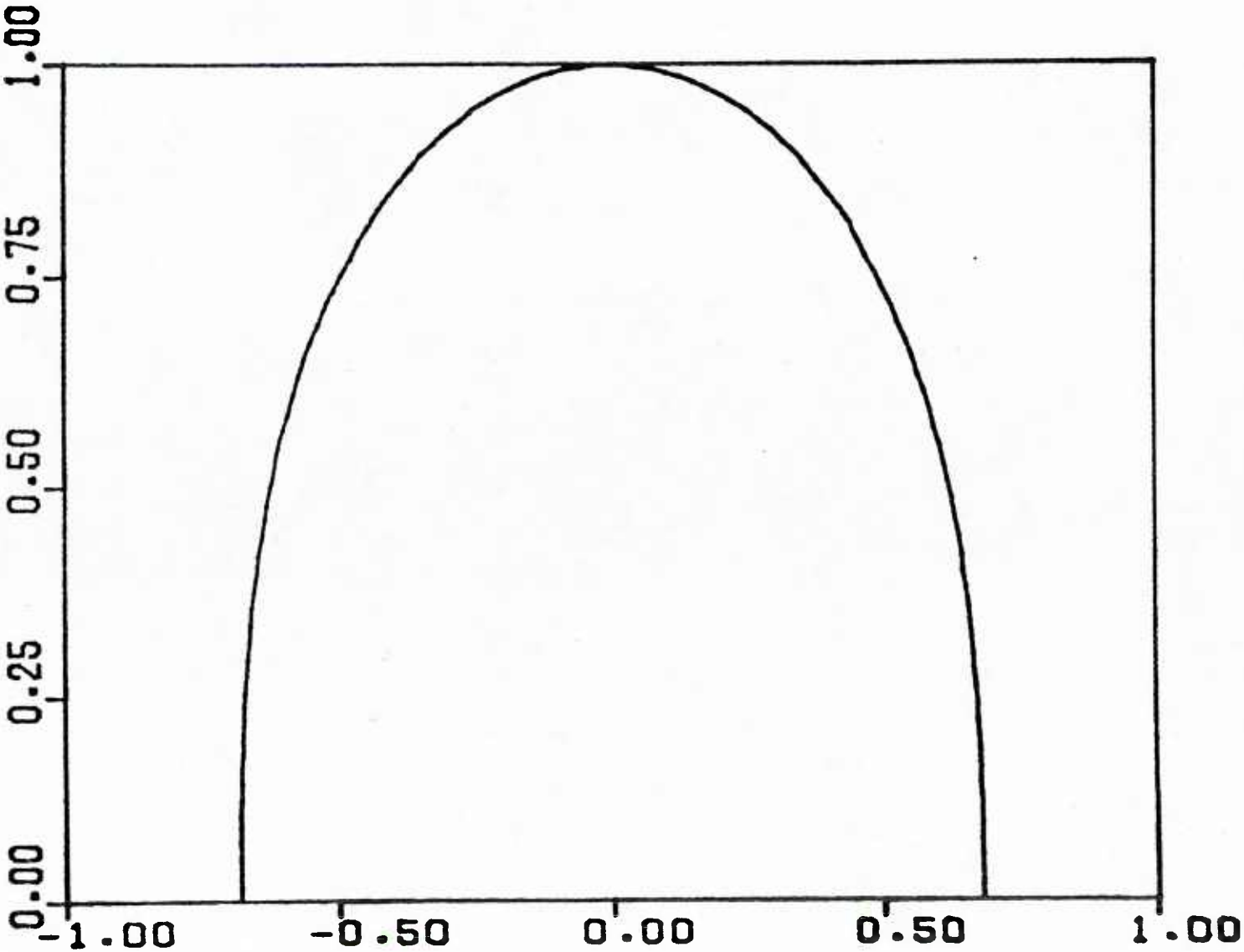

(a)

Figure 8: The radiation patterns of (a) the first,...,(e) fifth characteristic fields for a 0.4λ slot.

$|\underline{H}_3|$

(b)

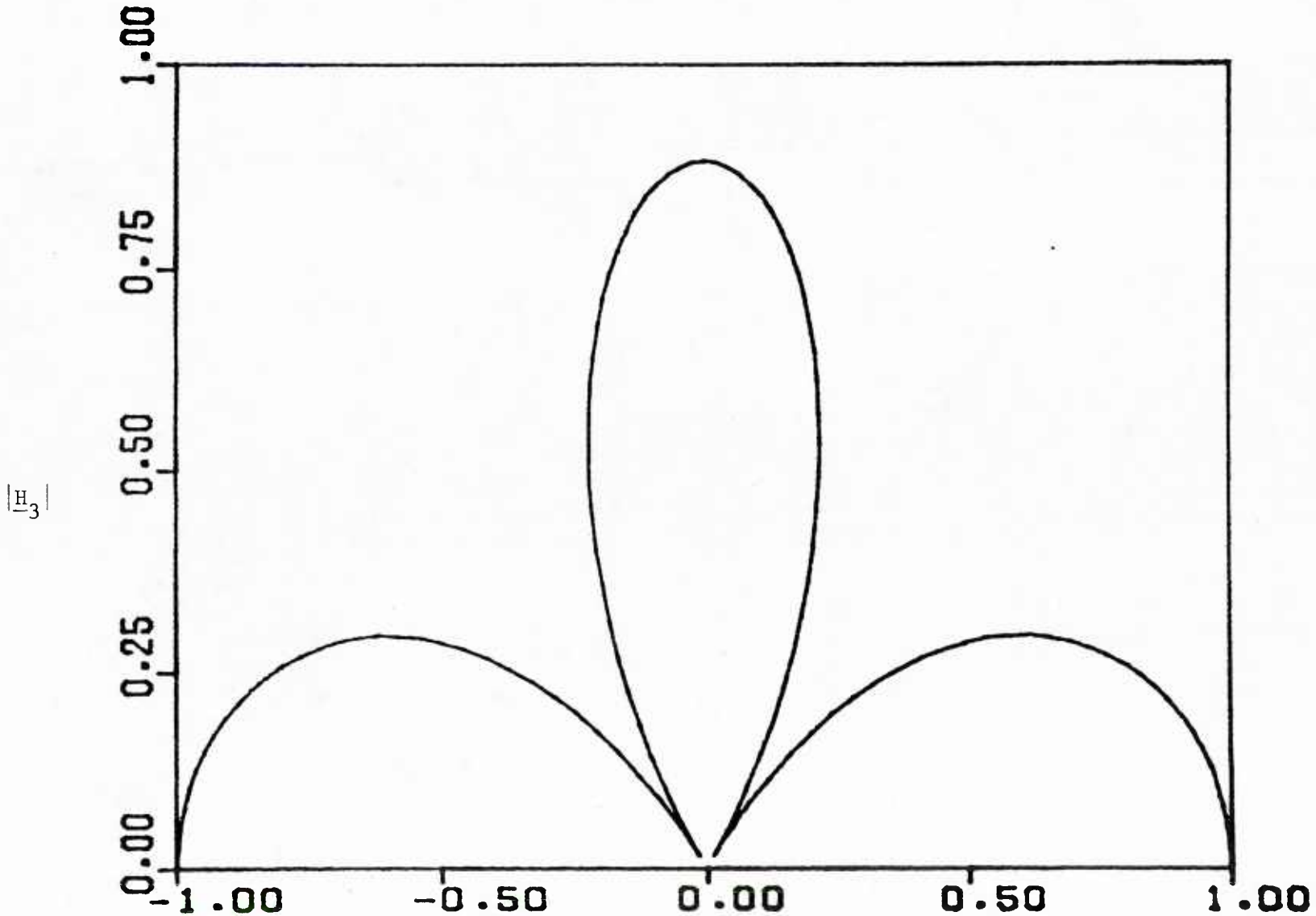

$|\underline{H}_3|$

(c)

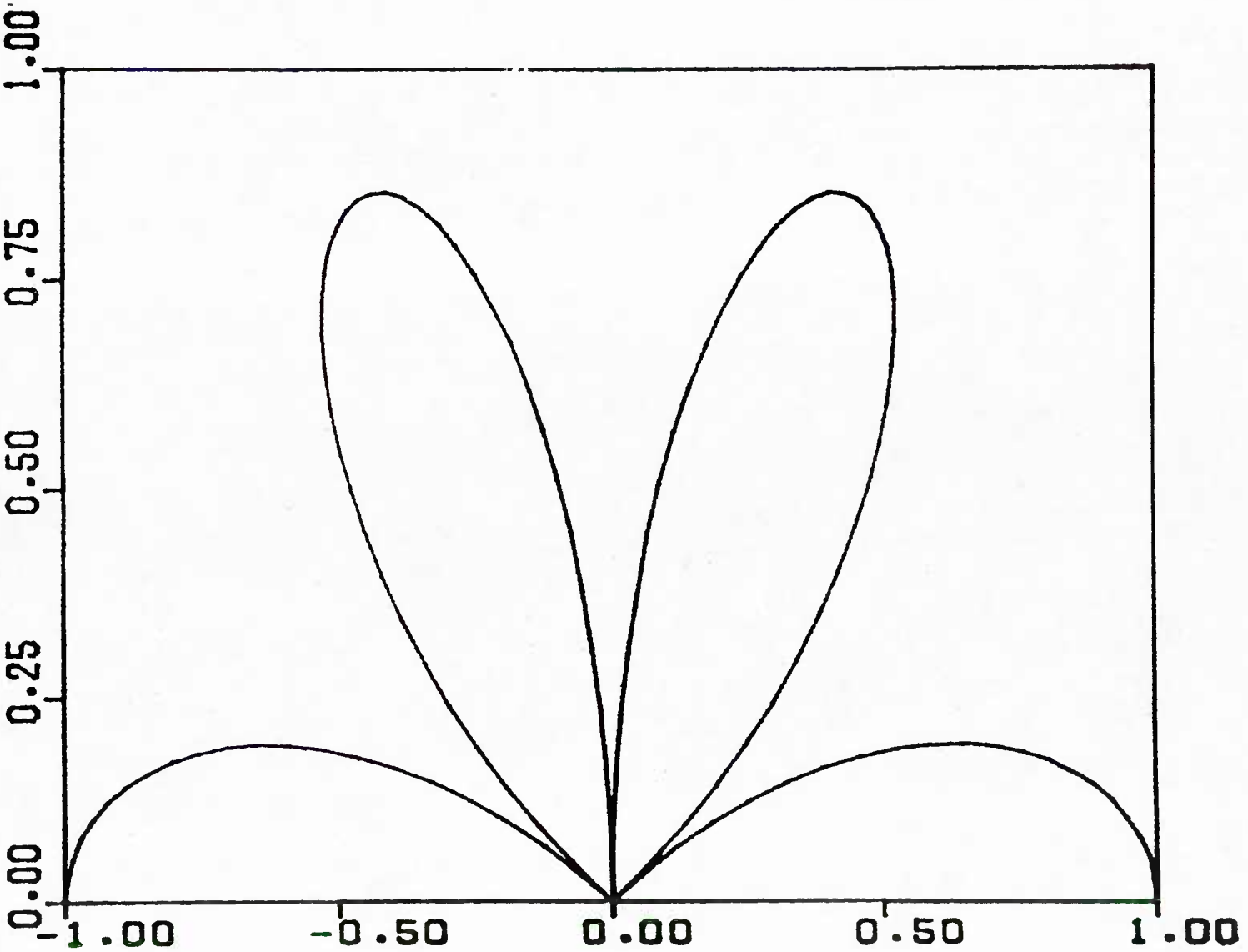

$|\underline{H}_4|$

(d)

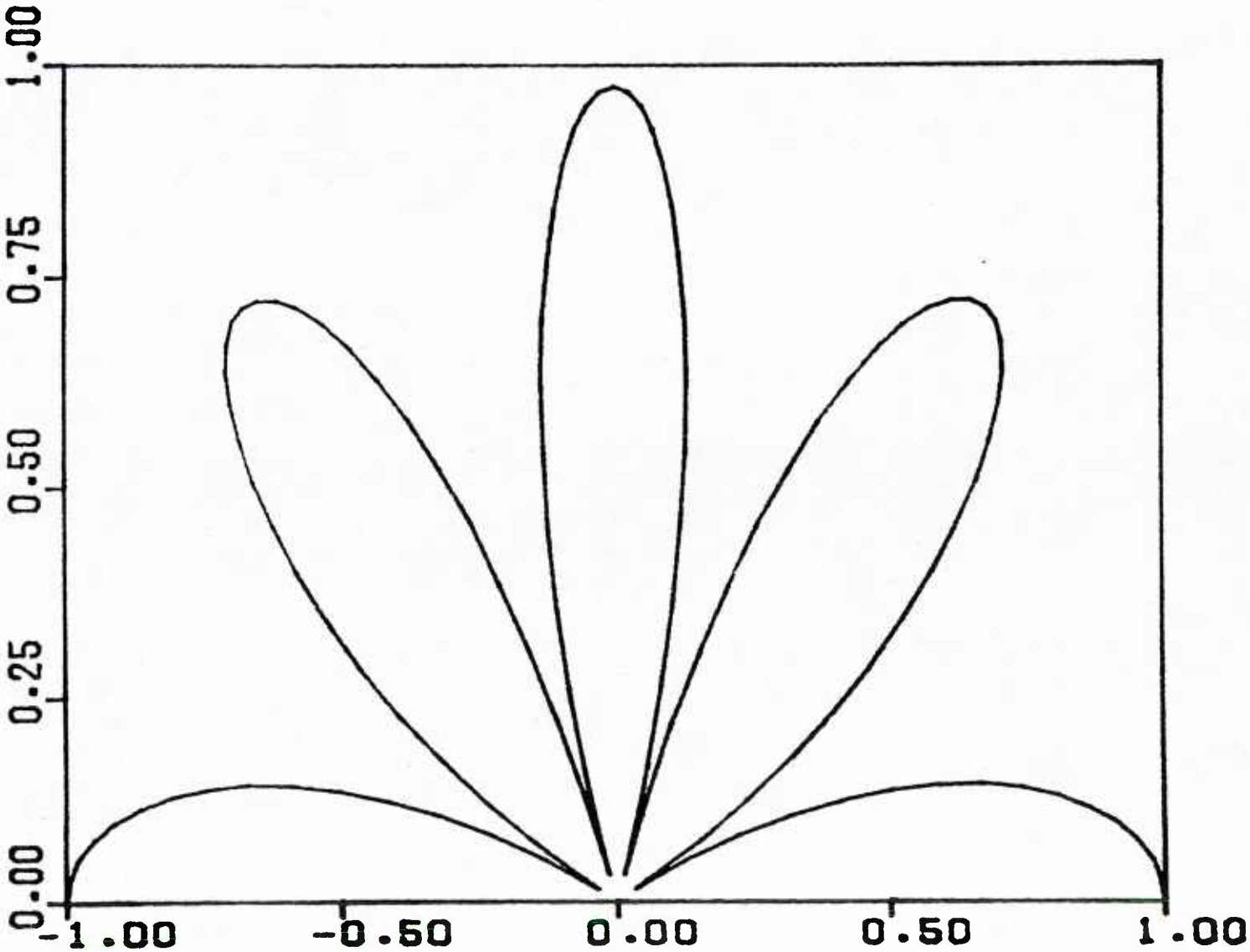

$|\underline{H}_5|$

(e)

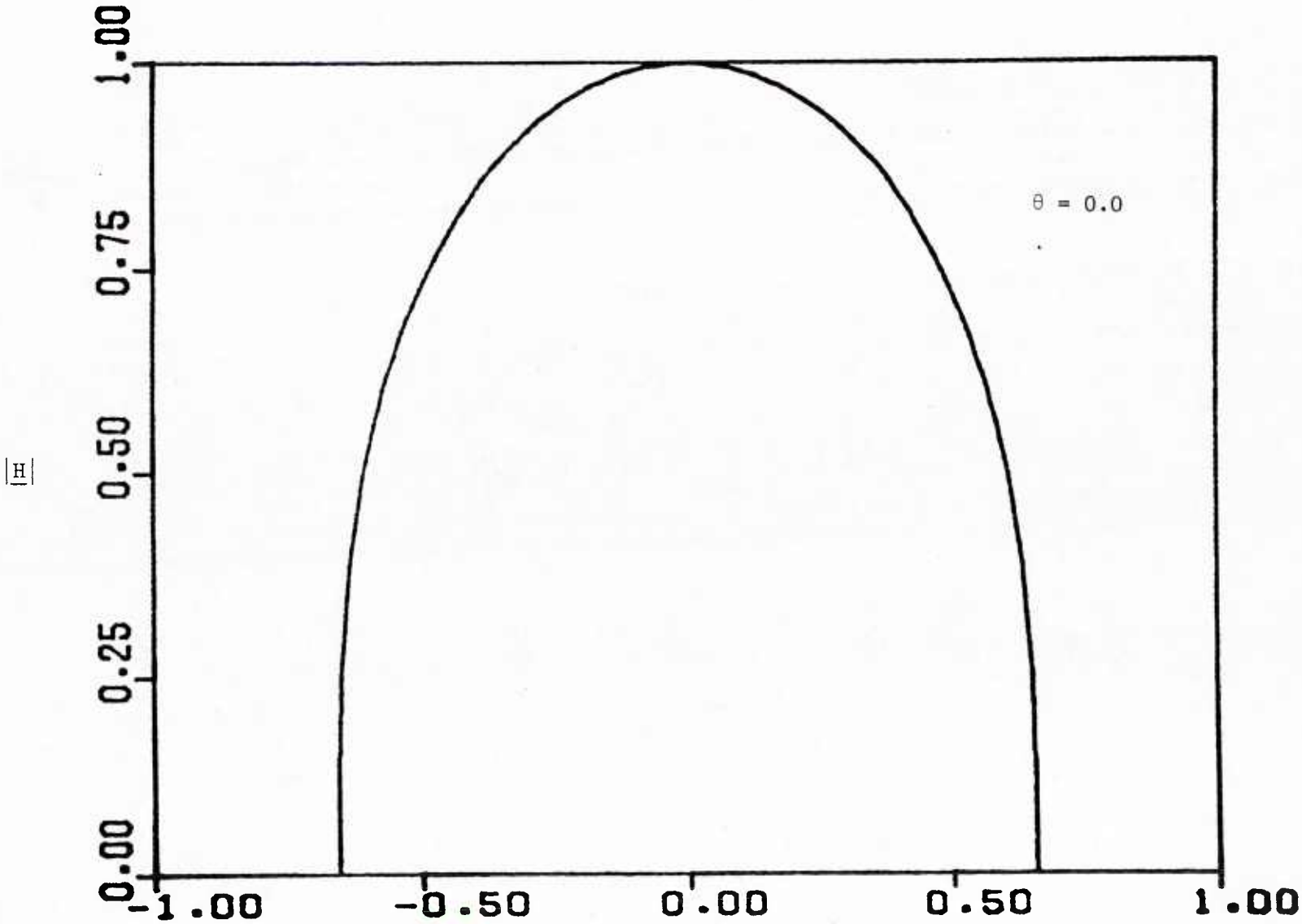

Figure 9: The radiation pattern for 0.4λ slot.

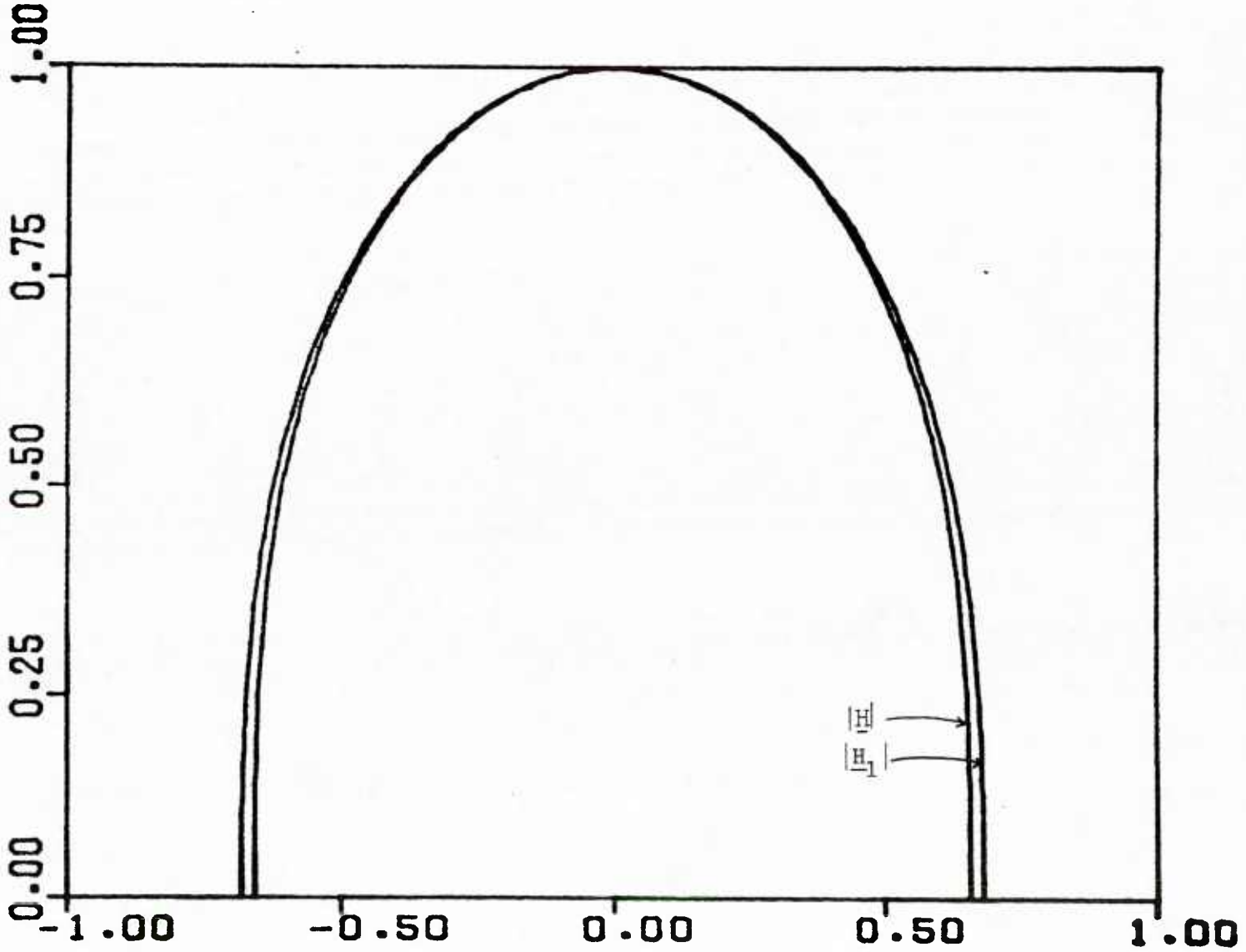

Figure 10: Comparison of the radiation pattern for a 0.4 λ slot (θ=0.0) to that of its dominant mode.

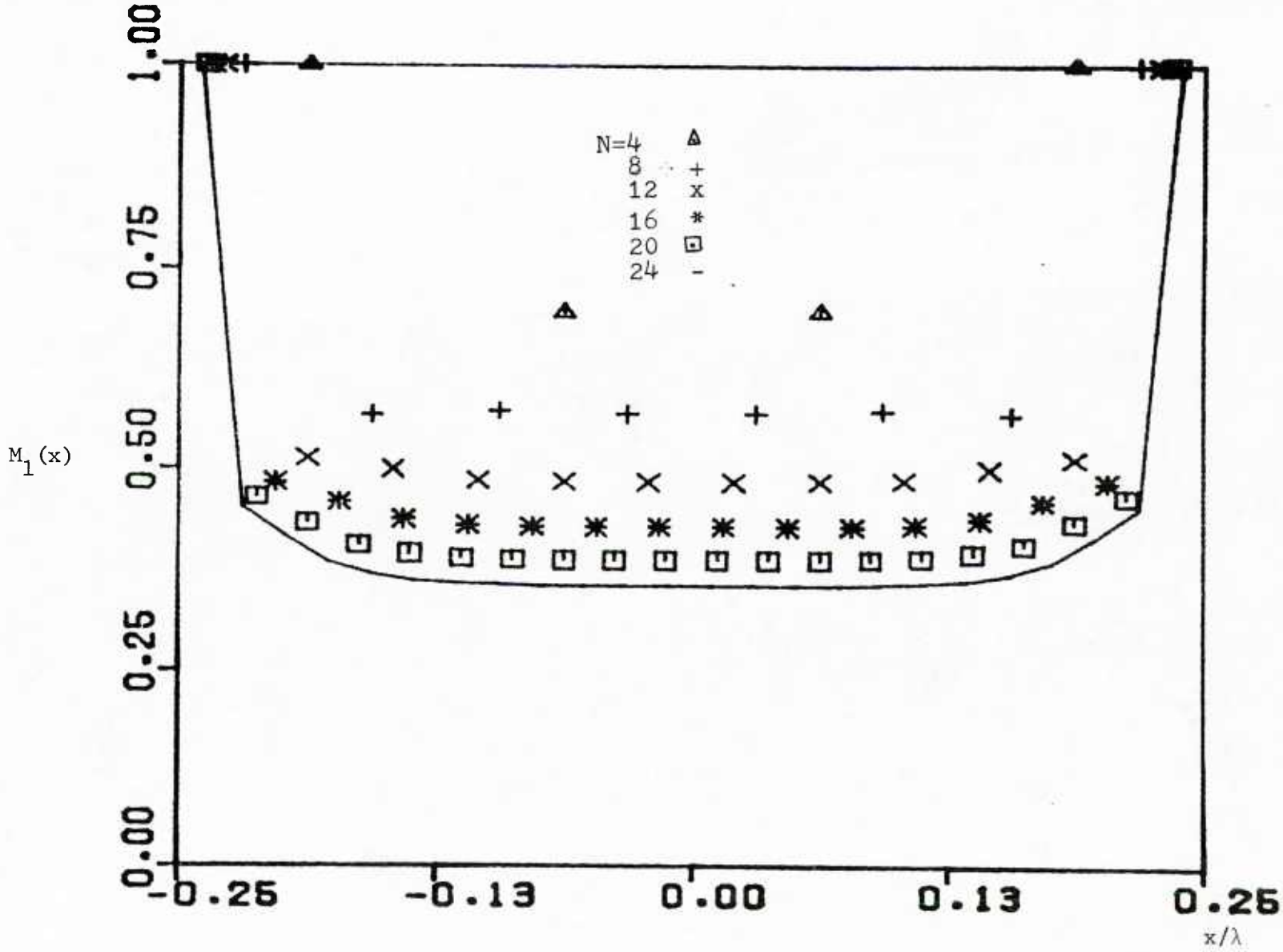

Figure 11: The convergence of the dominant characteristic current for a 0.5 λ slot normalized for a maximum amplitude of unity.

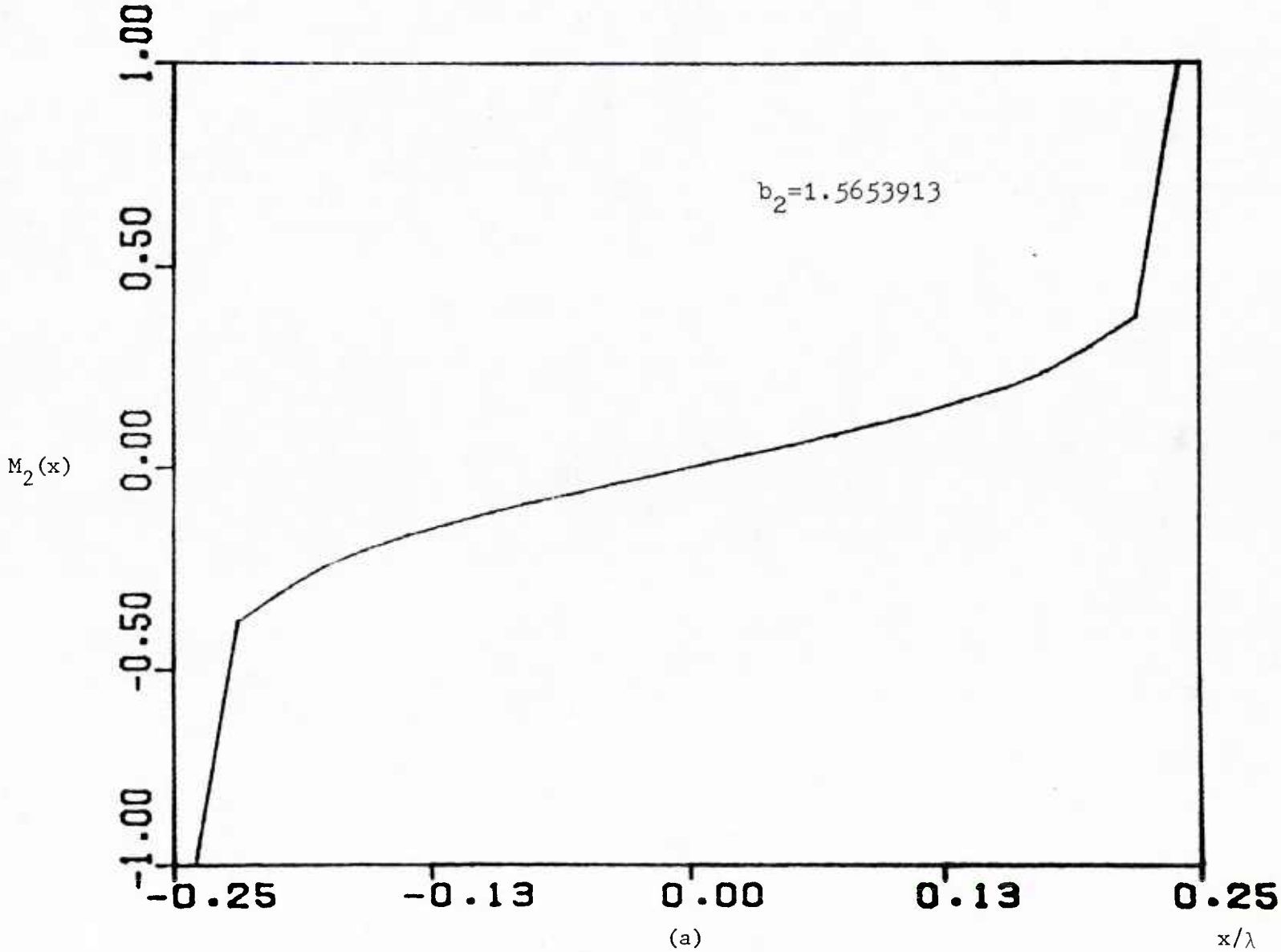

Figure 12: (a) The second,...,(d) fifth characteristic currents for a 0.5λ slot normalized for maximum amplitude of unity.

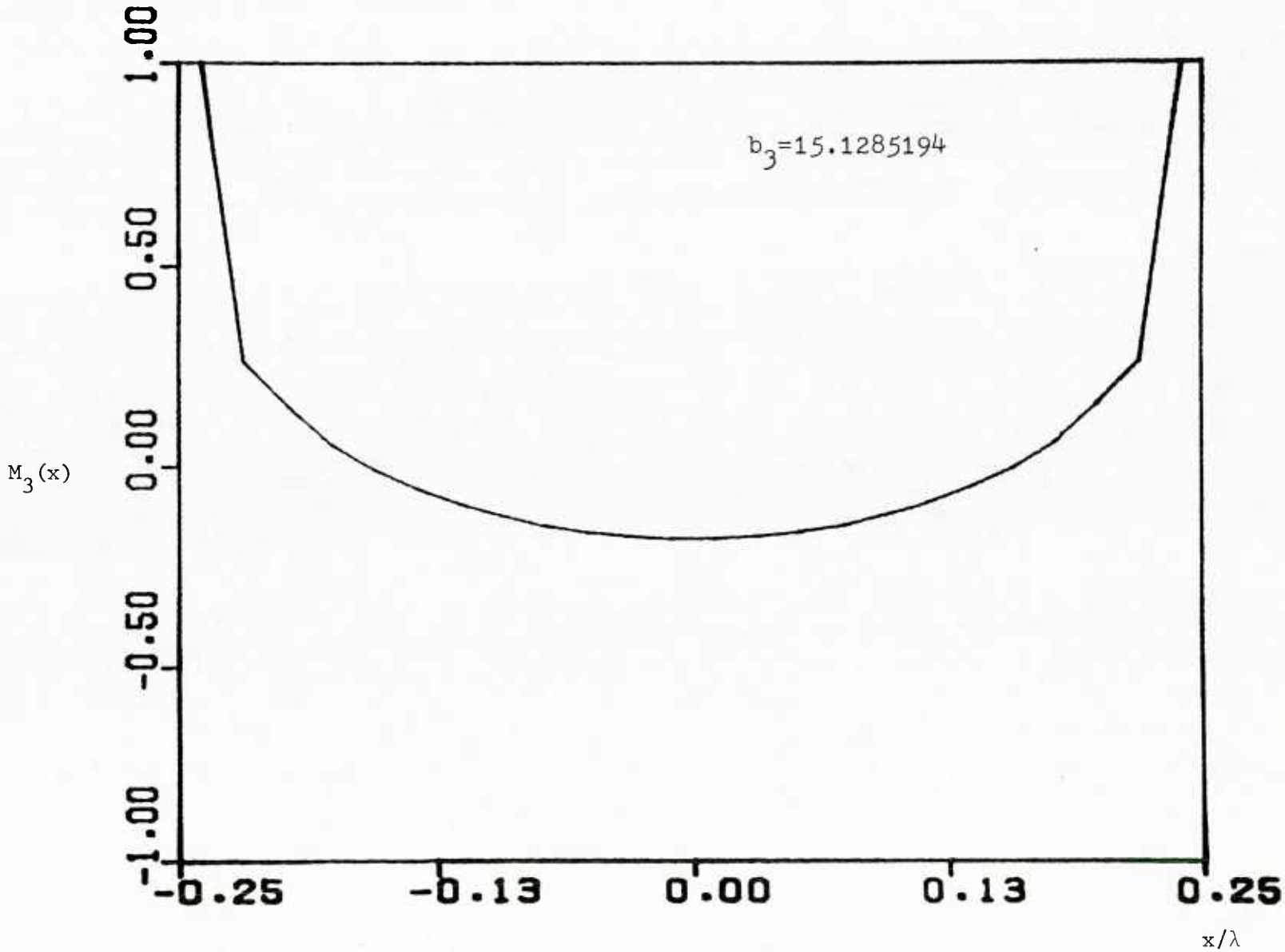

(b)

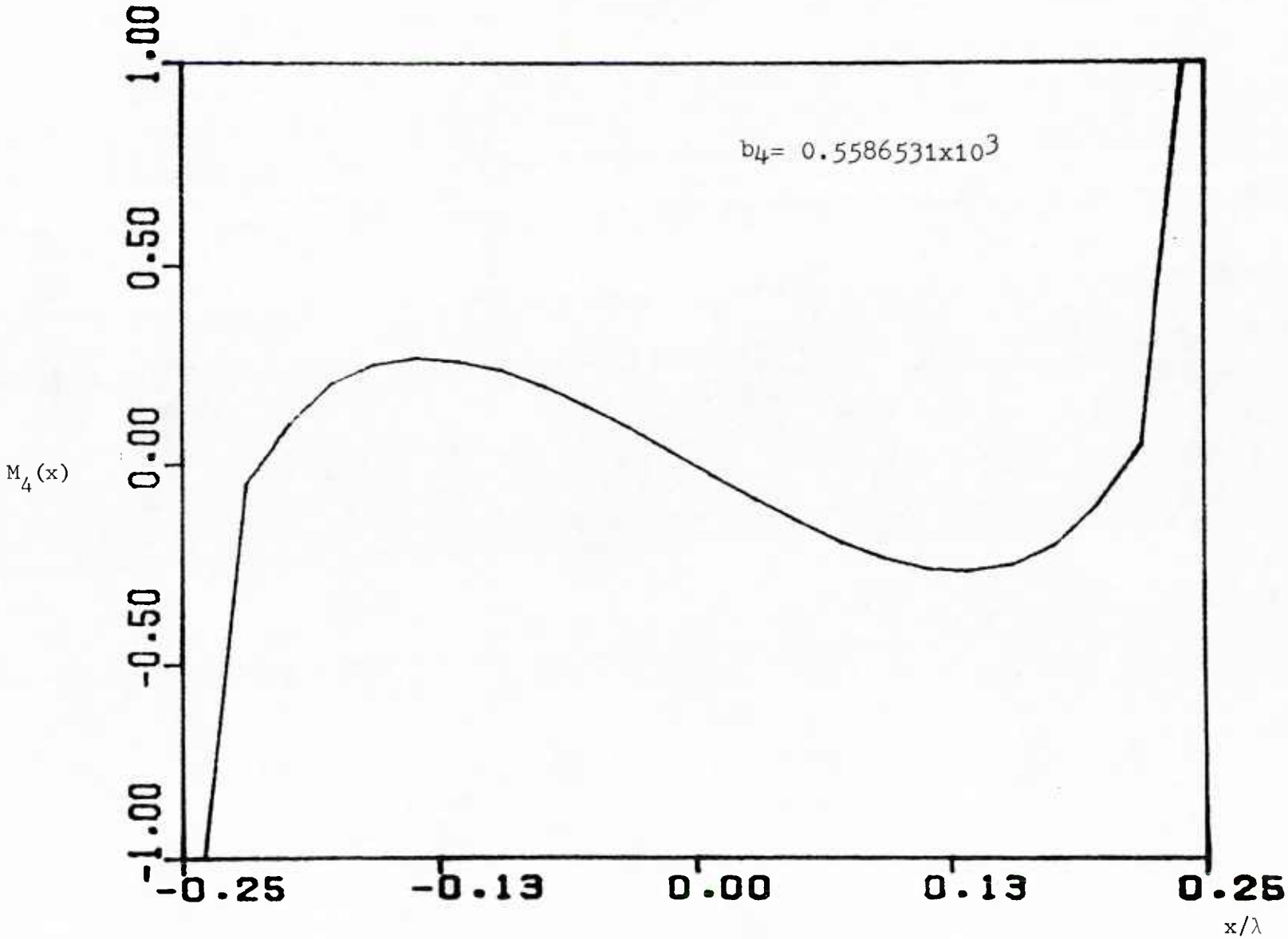

(c)

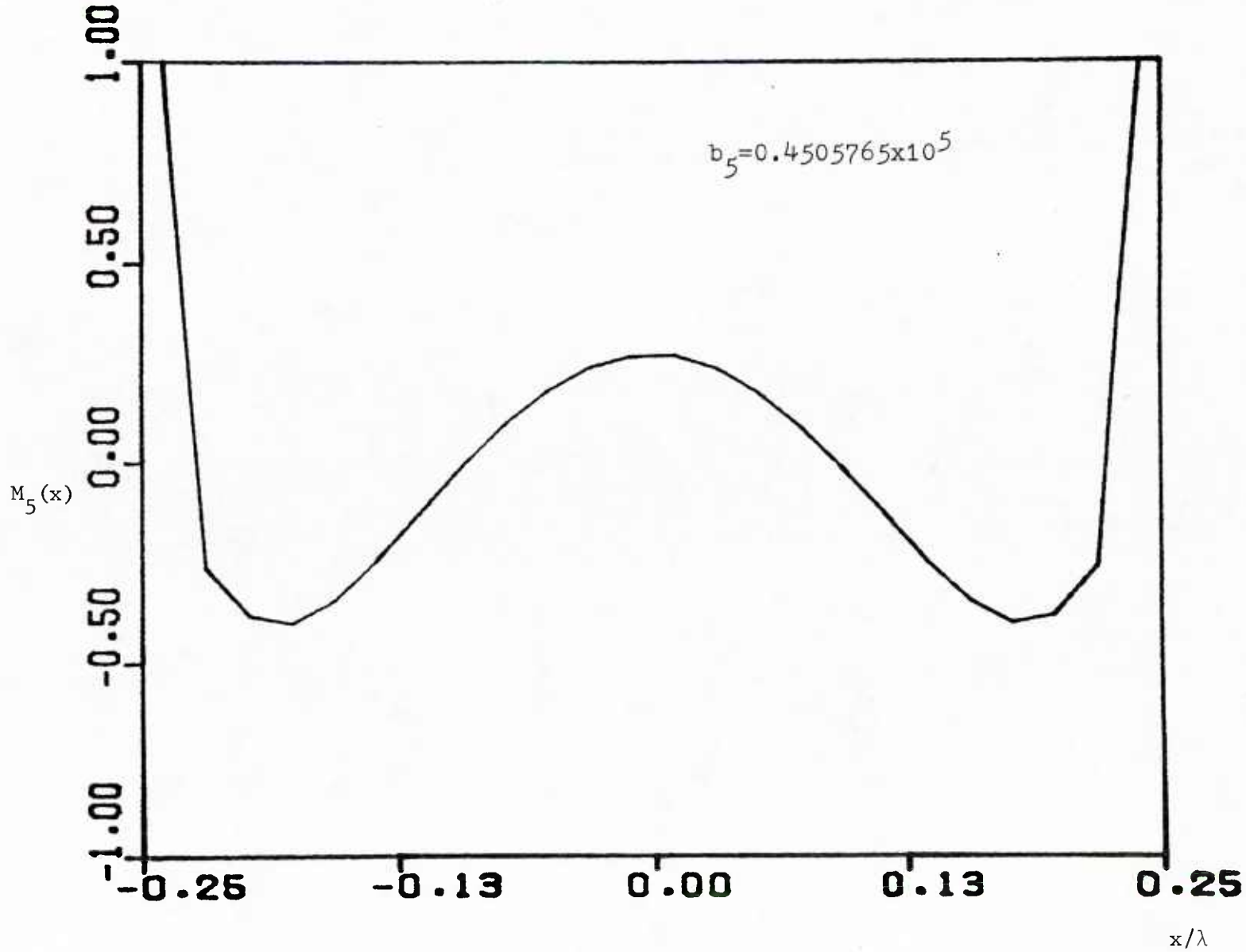

(d)

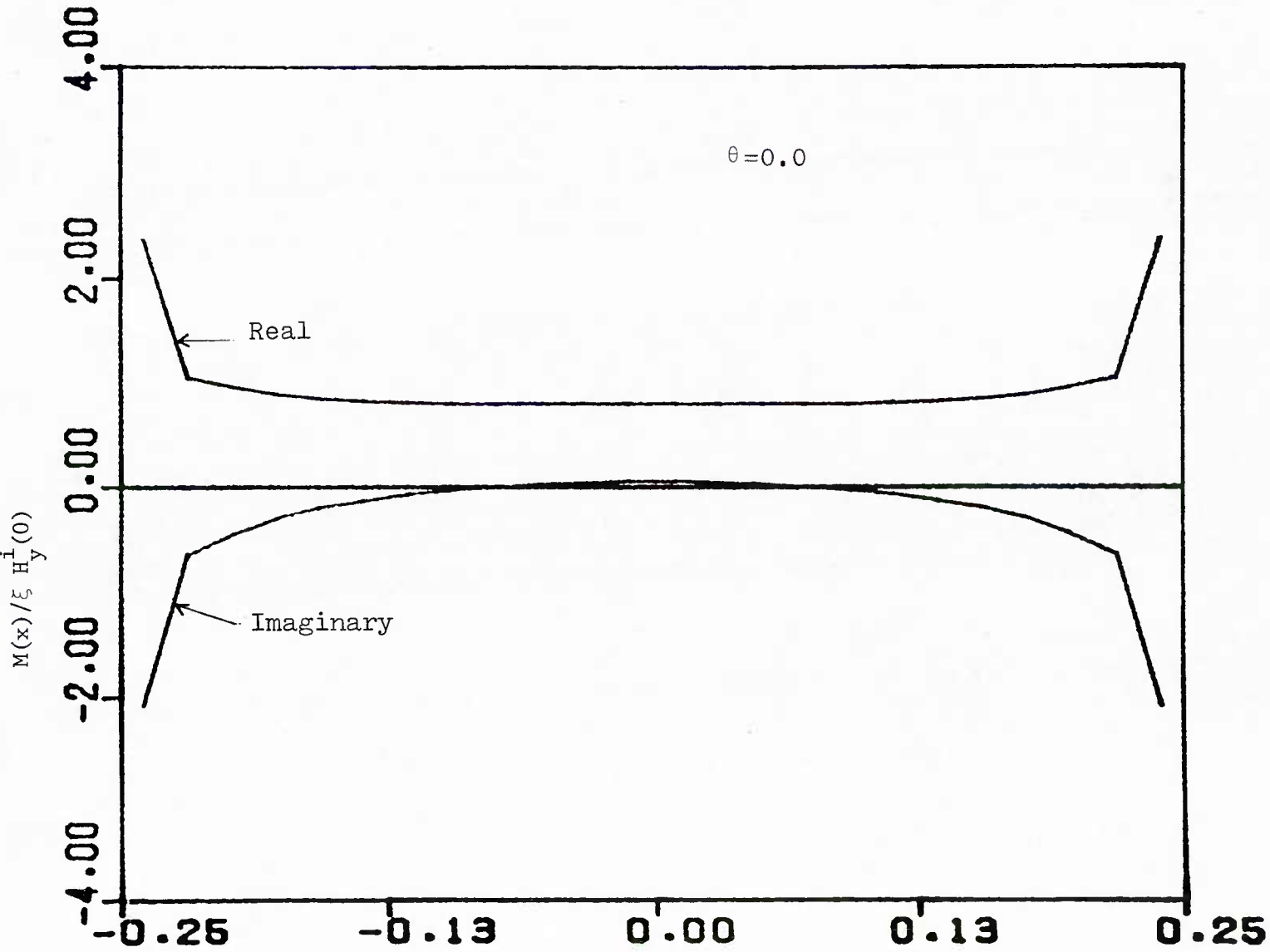

Figure 13: The equivalent magnetic current for a 0.5λ slot. Only the (5) physical characteristic currents are used in the summation.

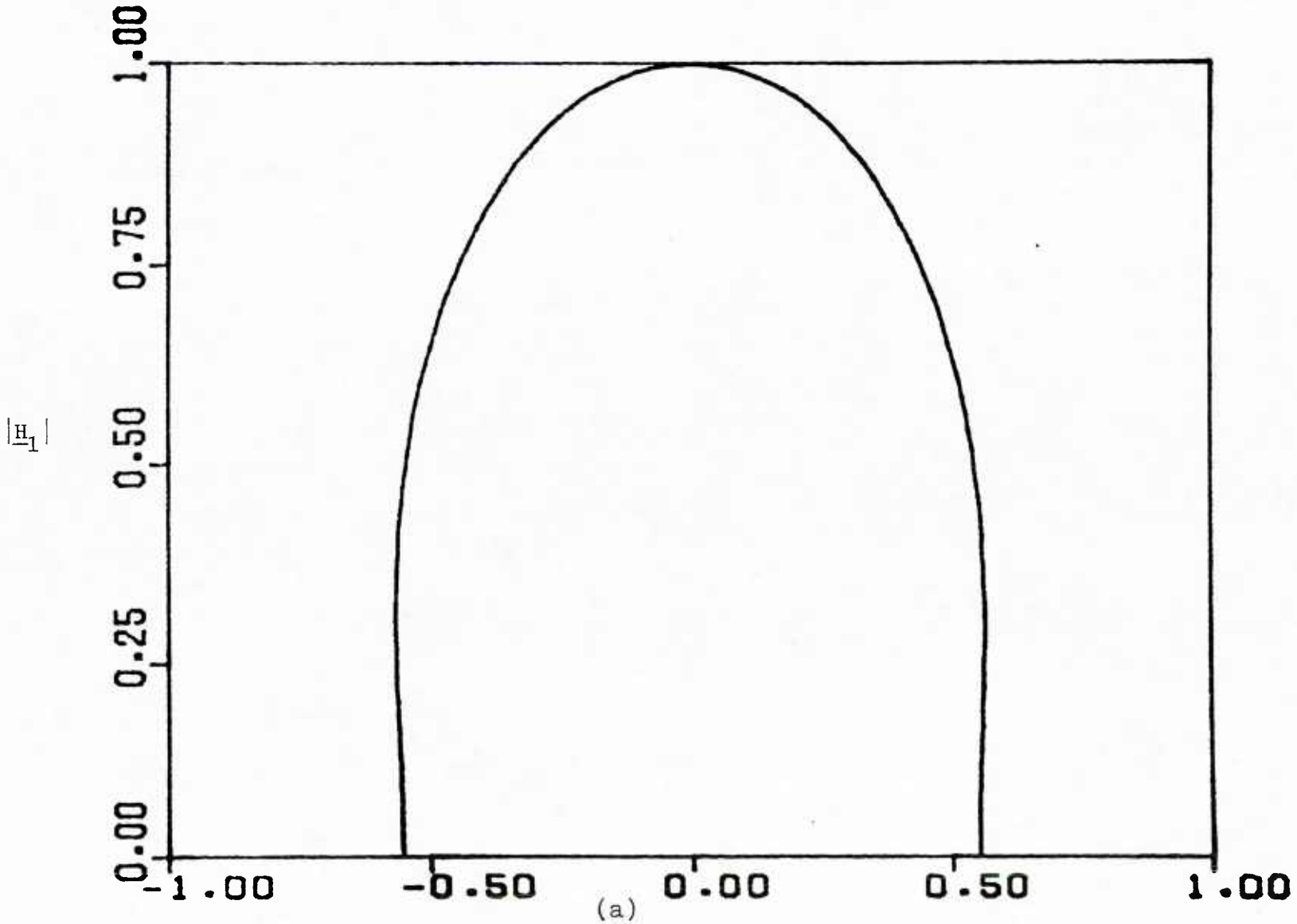

Figure 14: The radiation patterns of (a) the first,...,(e) fifth characteristic fields for a 0.5λ slot.

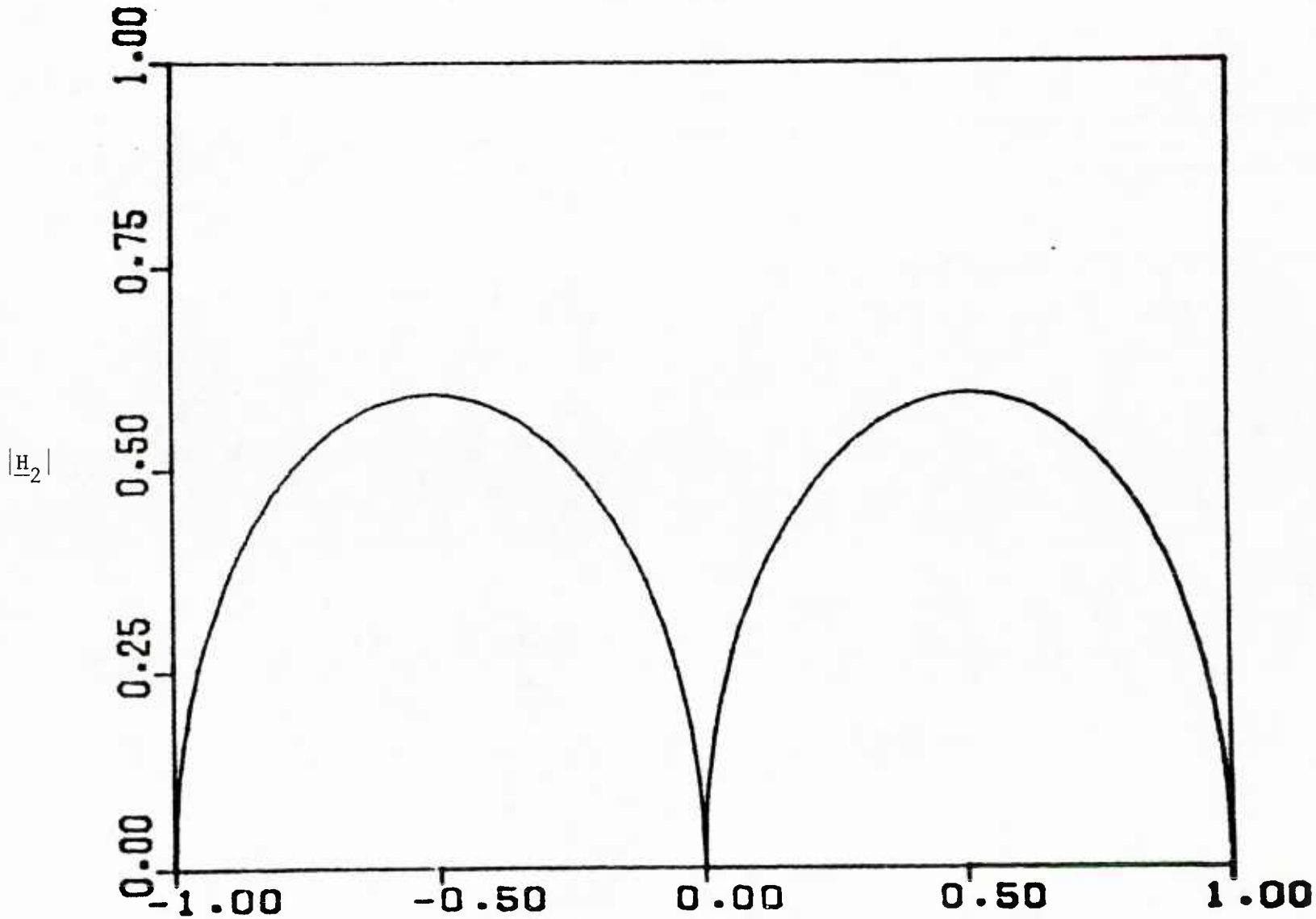

(b)

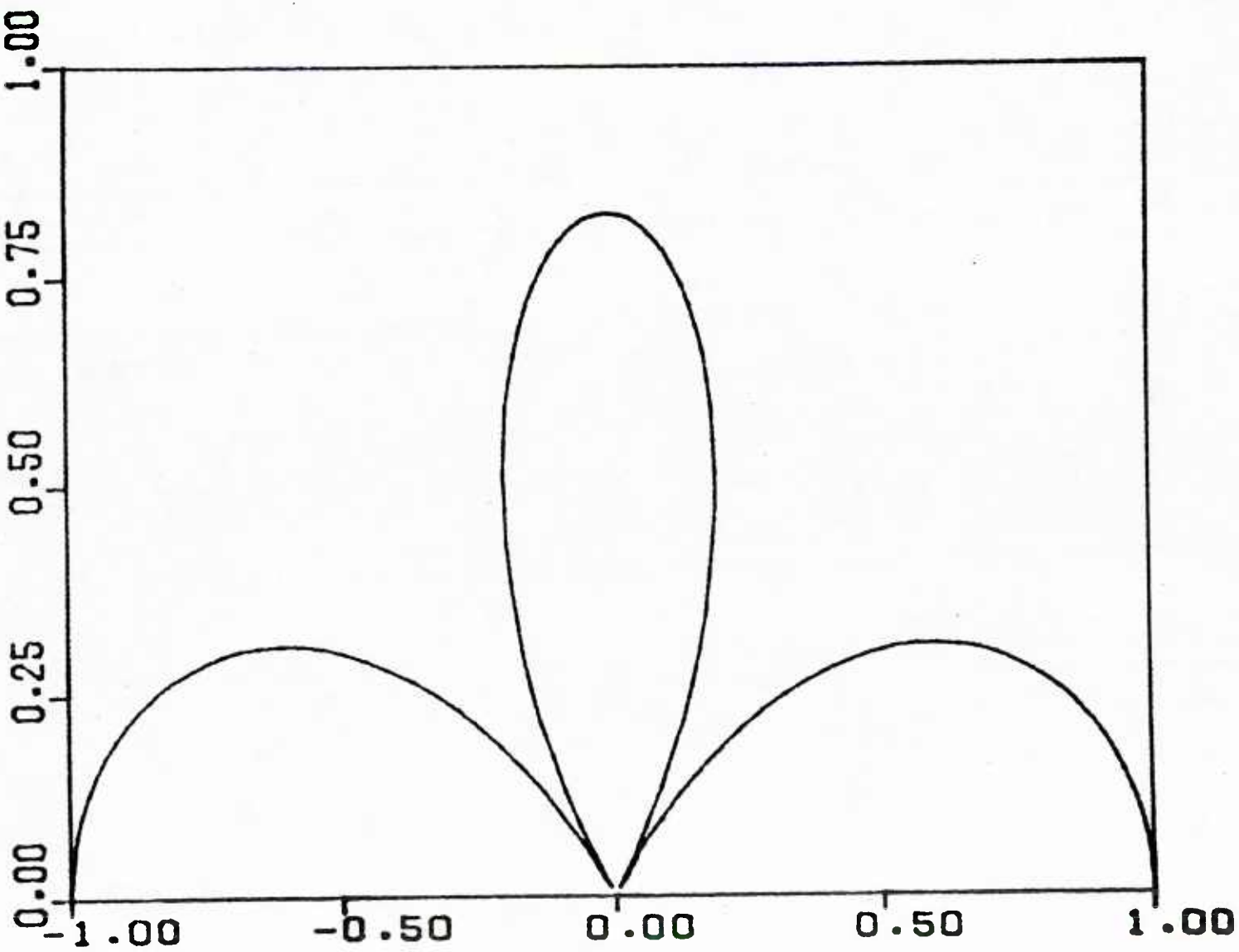

$|\underline{H}_3|$

(c)

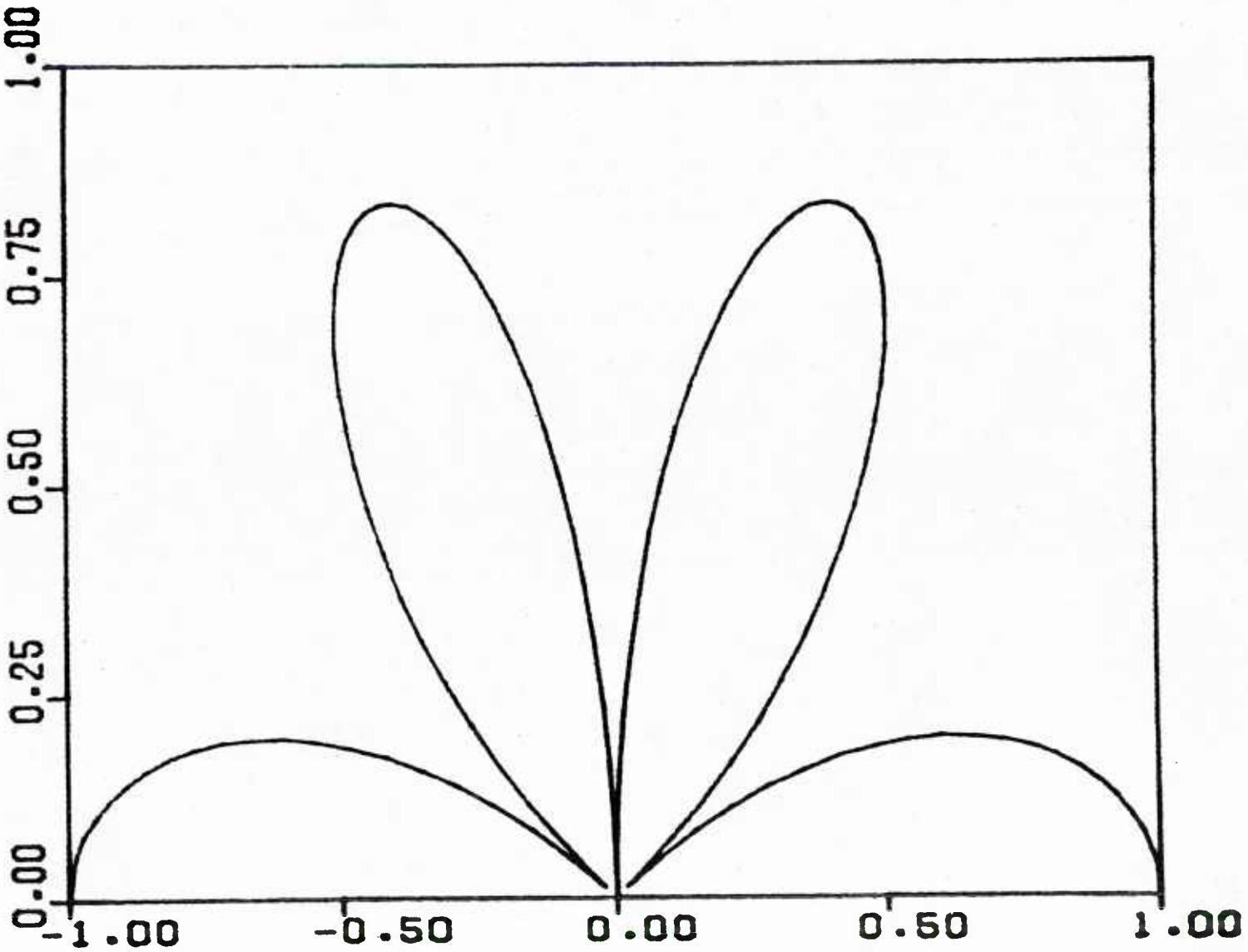

$|\underline{H}_4|$

(d)

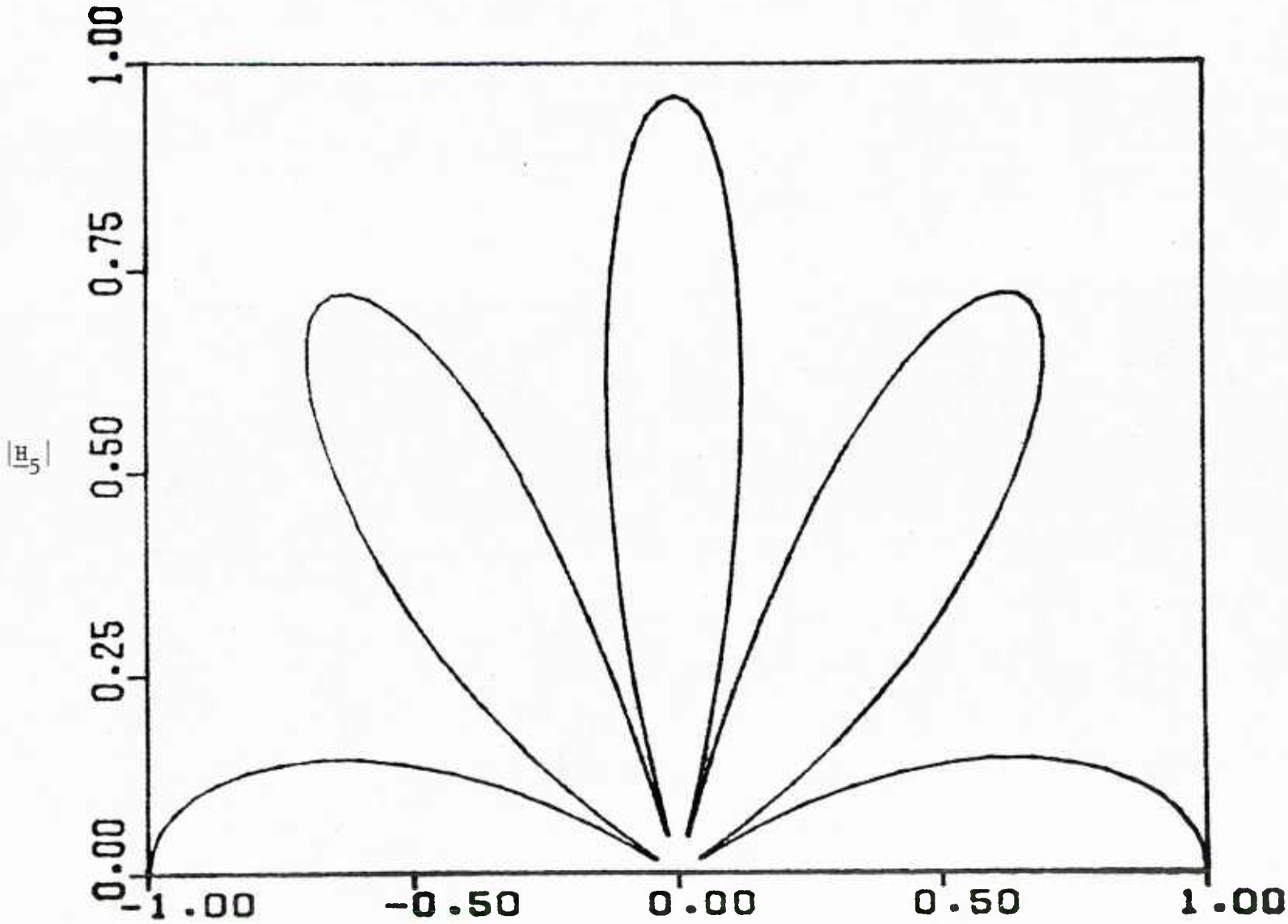

(e)

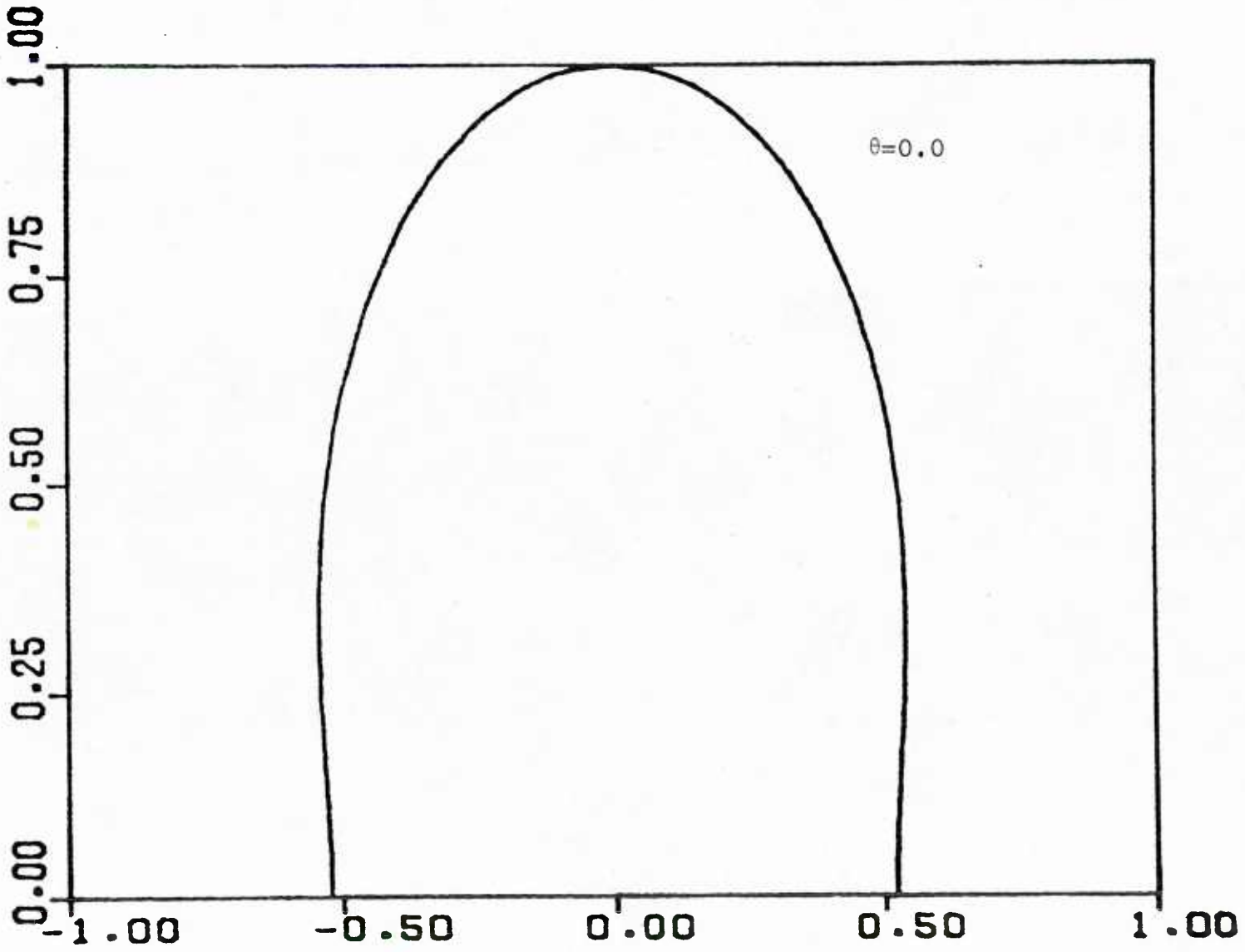

Figure 15: The radiation pattern for a 0.5λ slot.

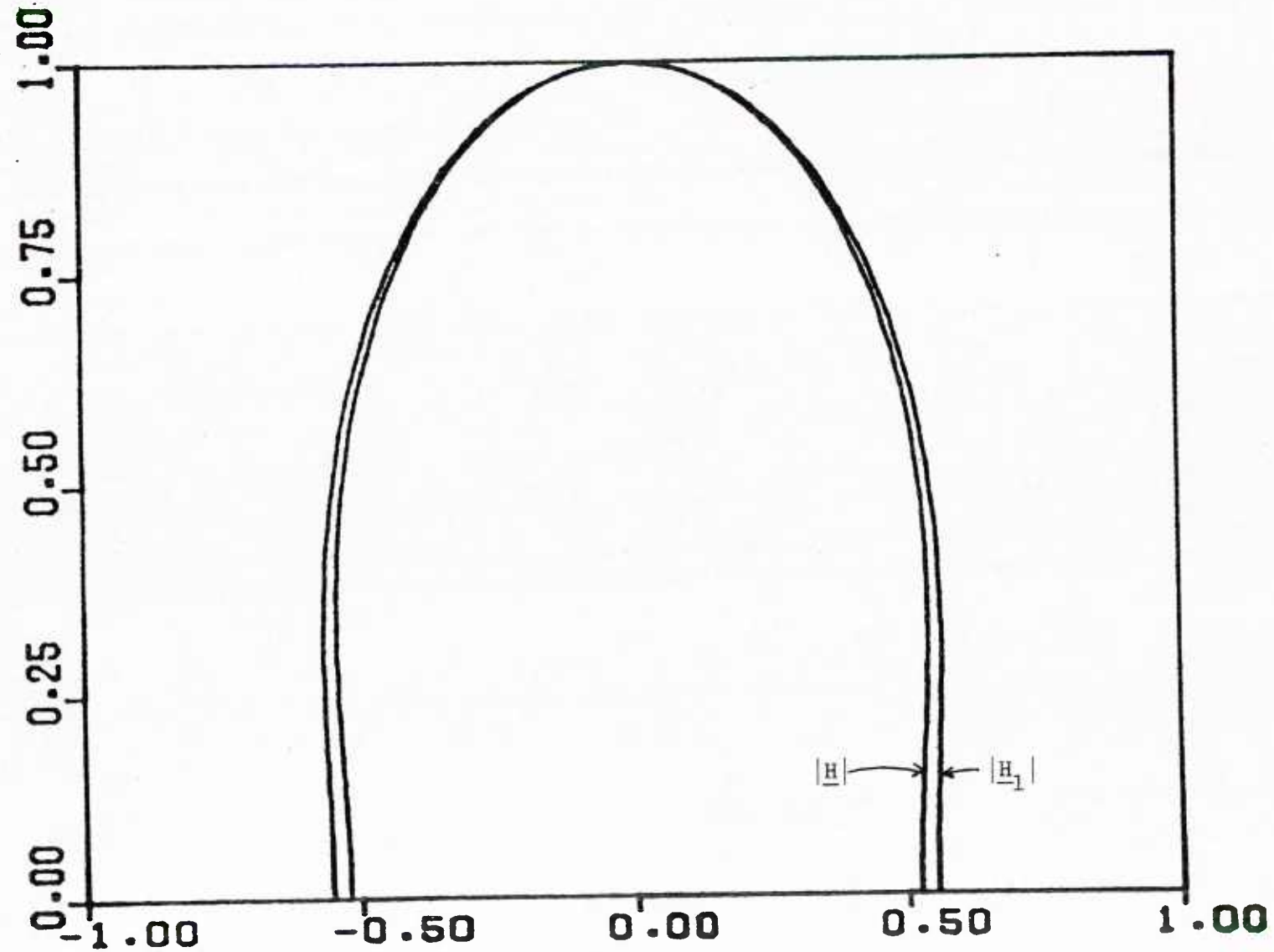

Figure 16: Comparison of the radiation pattern for a 0.5λ slot ($\theta = 0.0$) to that of its dominant characteristic field.

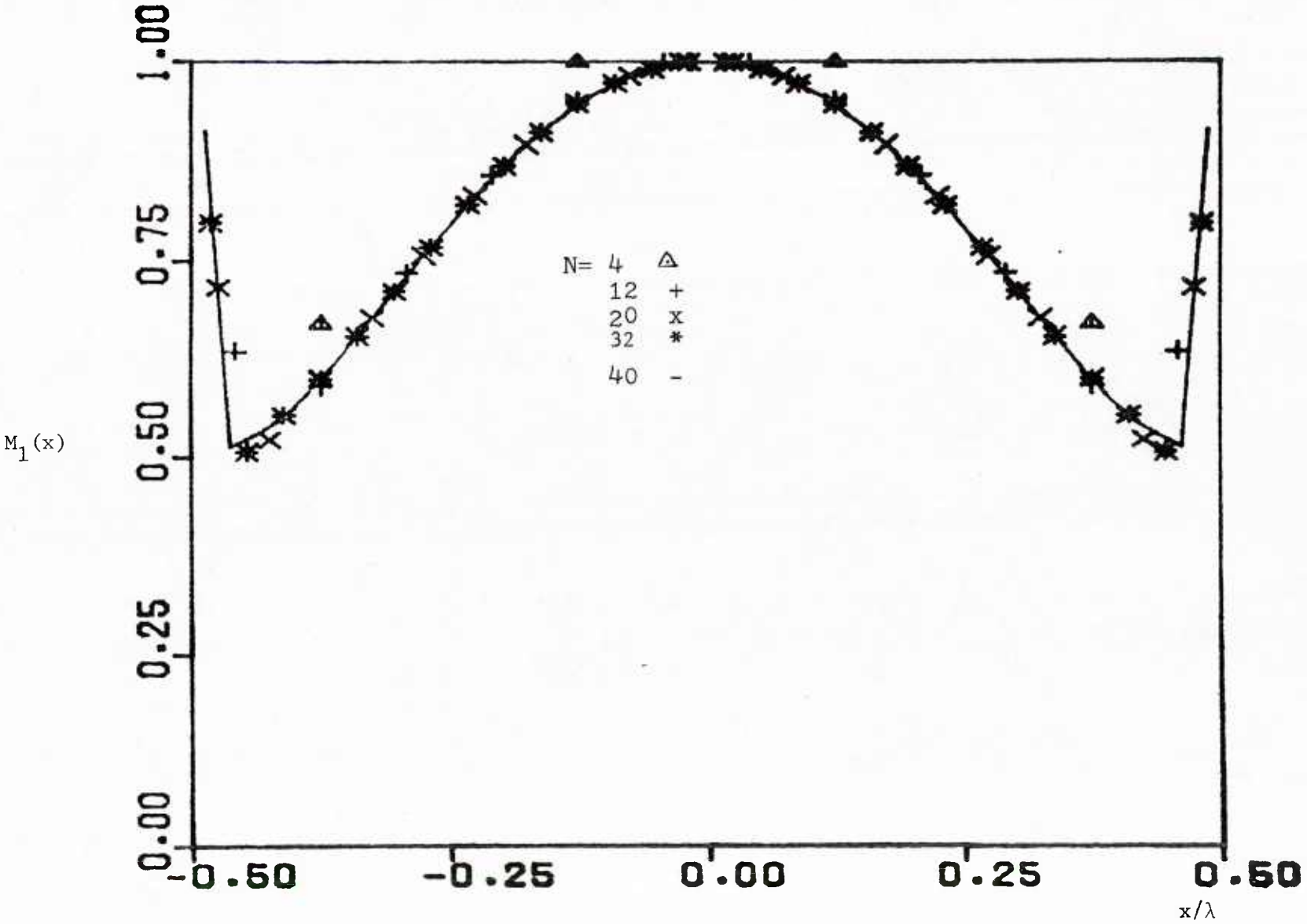

Figure 17: The convergence of the dominant chracteristic current for a 1.0λ slot normalized for a maximum amplitude of unity.

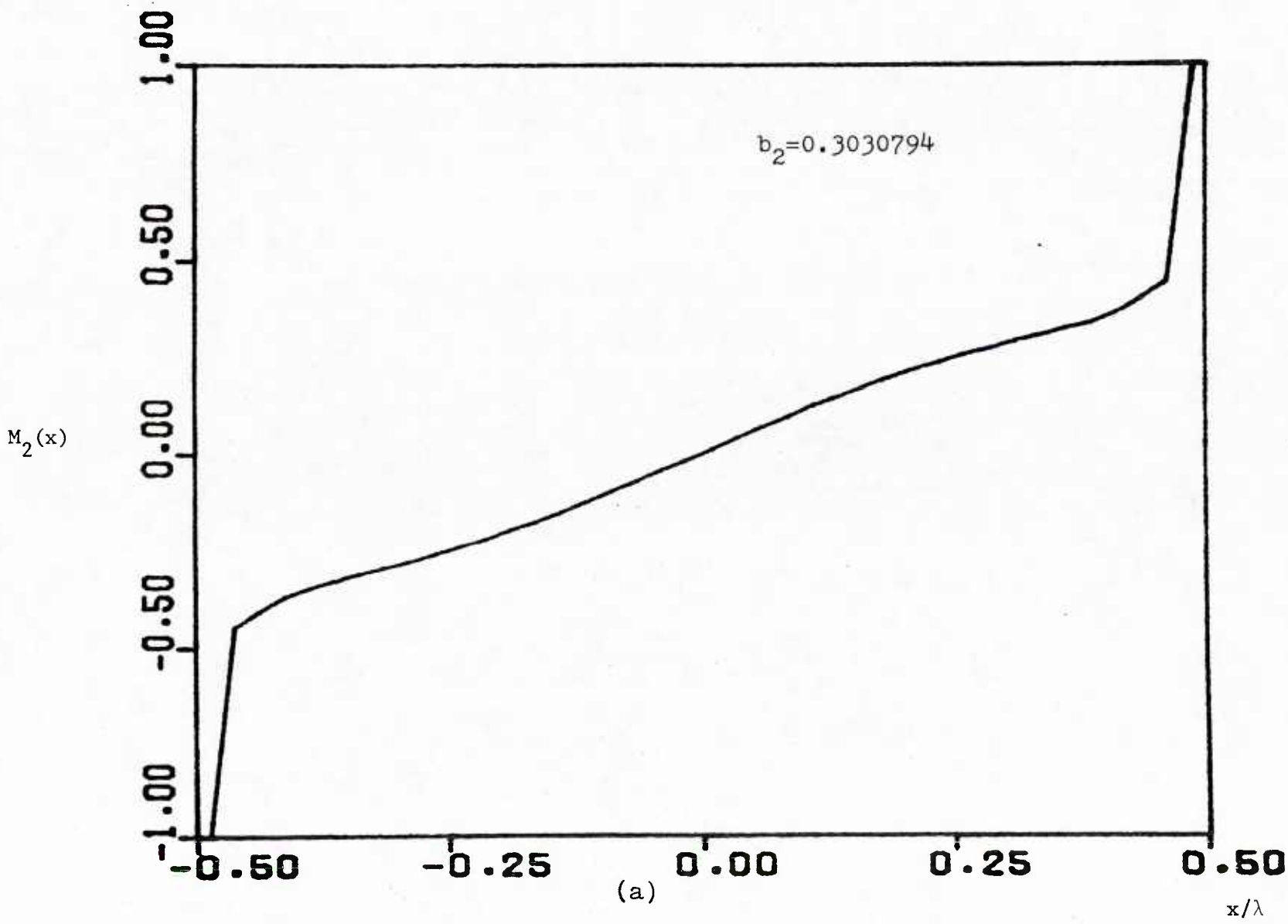

Figure 18: (a) The second,...,(f) the seventh characteristic currents for a 1.0λ slot normalized for a maximum amplitude of unity.

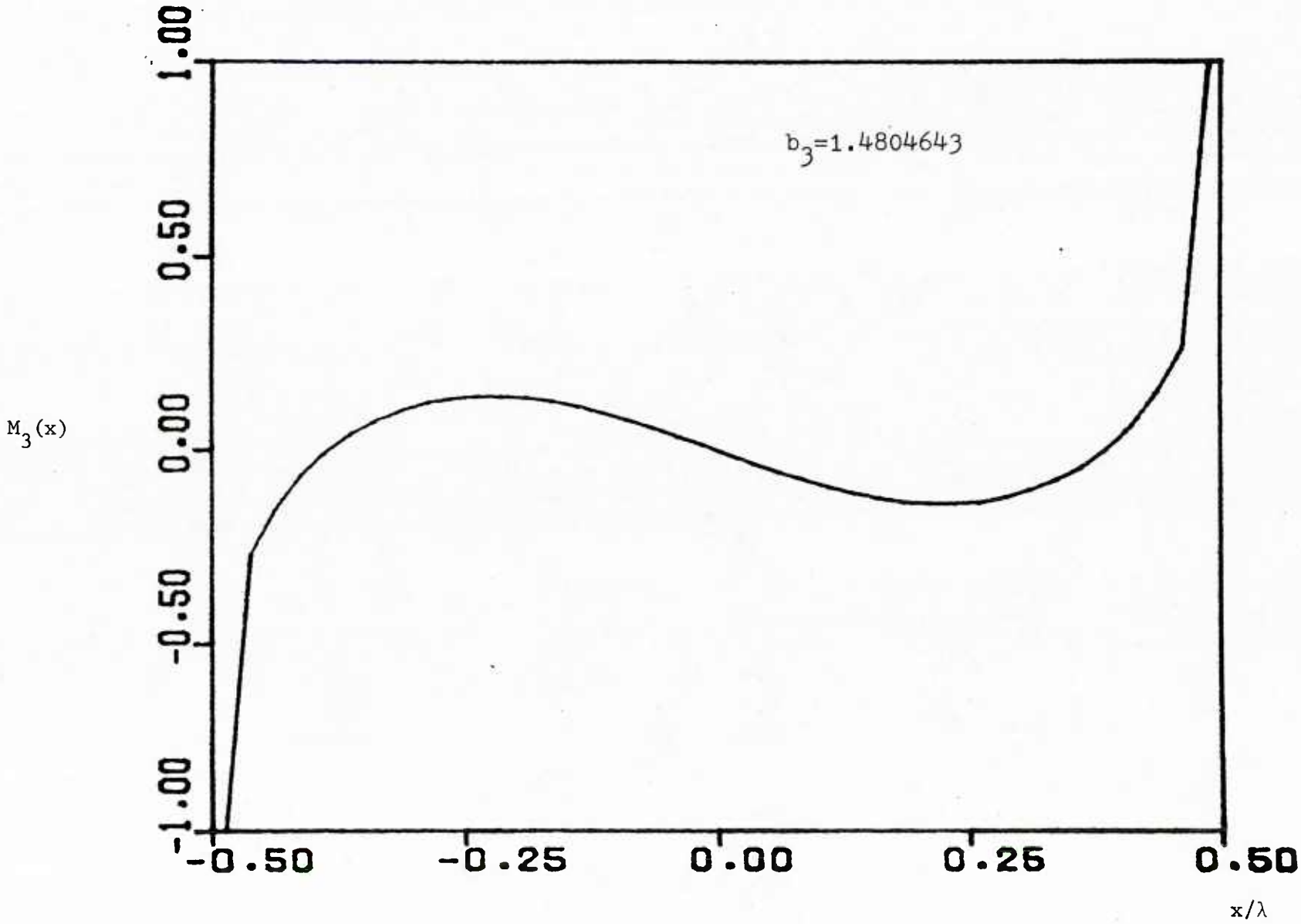

(b)

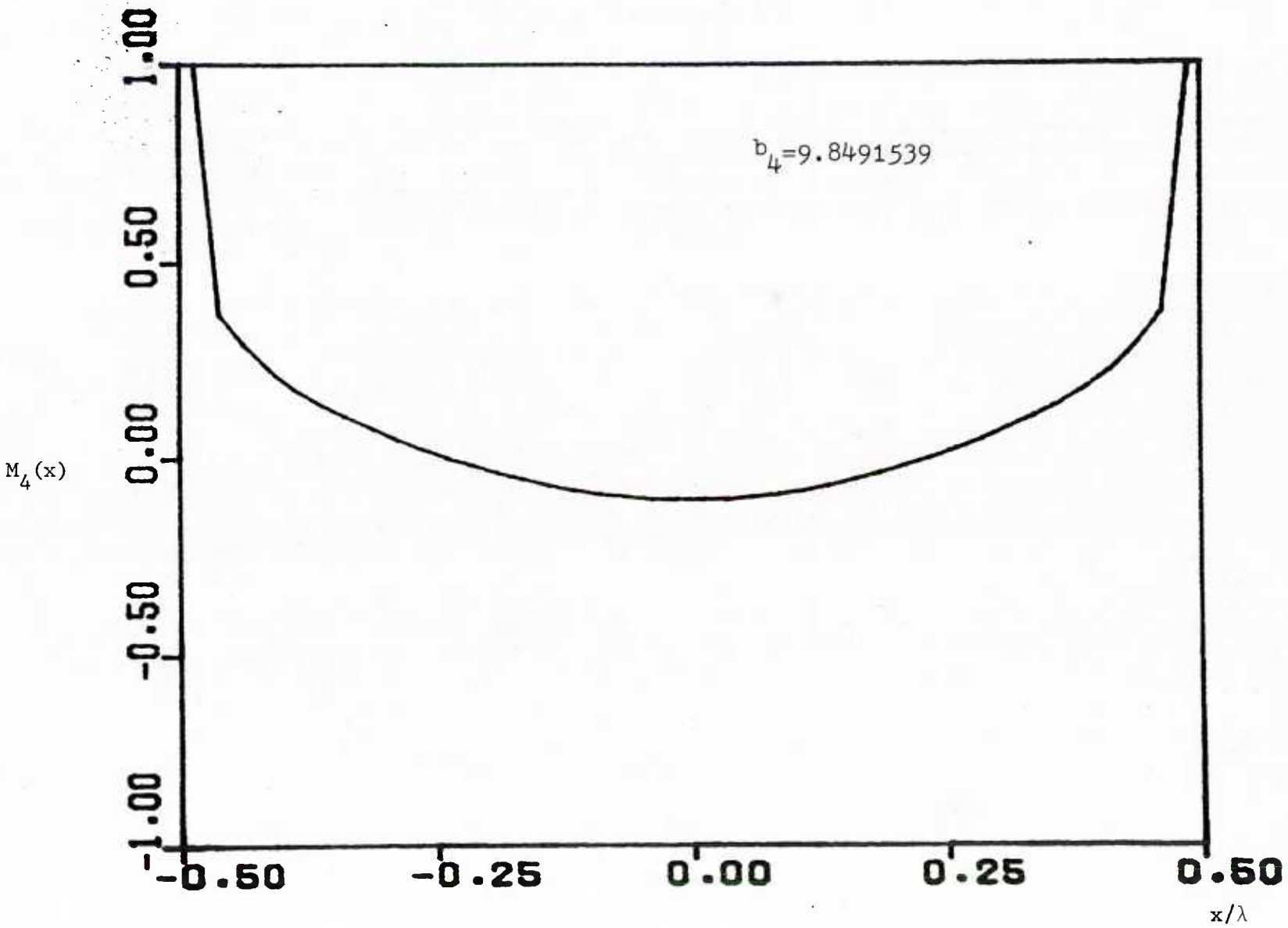

(c)

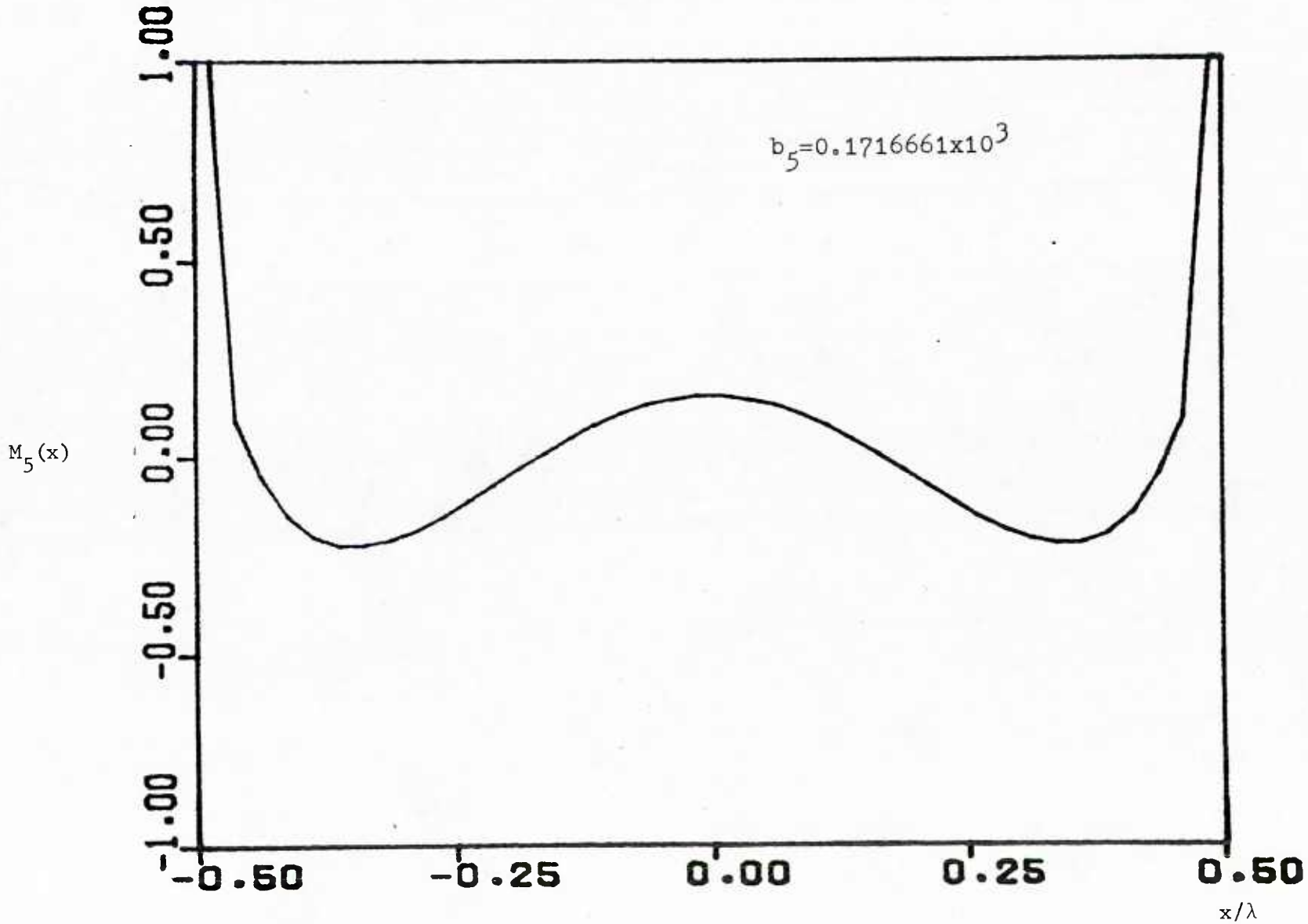

(d)

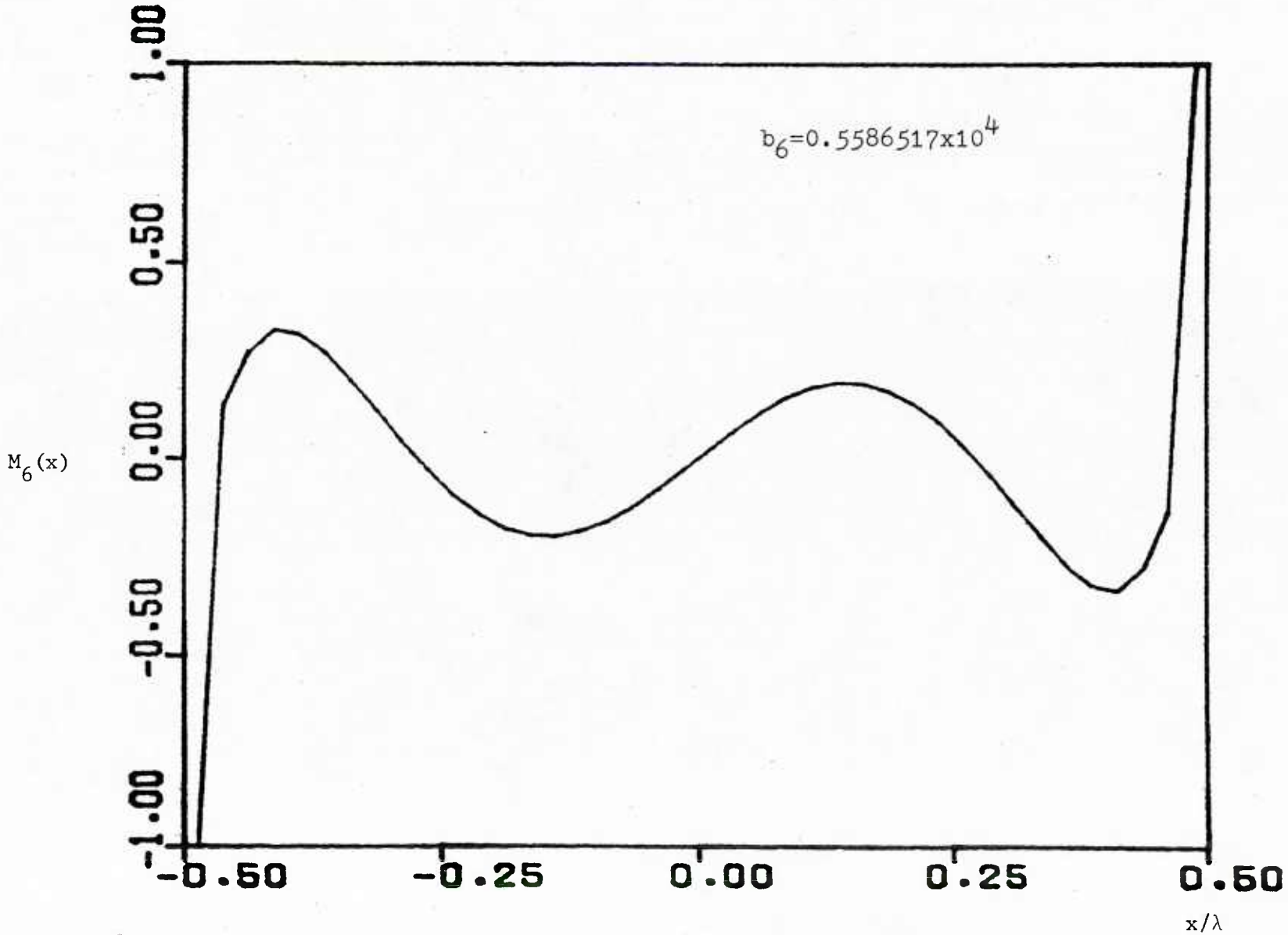
$b_6=0.5586517x10^4$
$M_6(x)$
1.00
0.50
0.00
-0.50
-1.00
-0.50
-0.25
0.00
0.25
0.50
x/λ

(e)

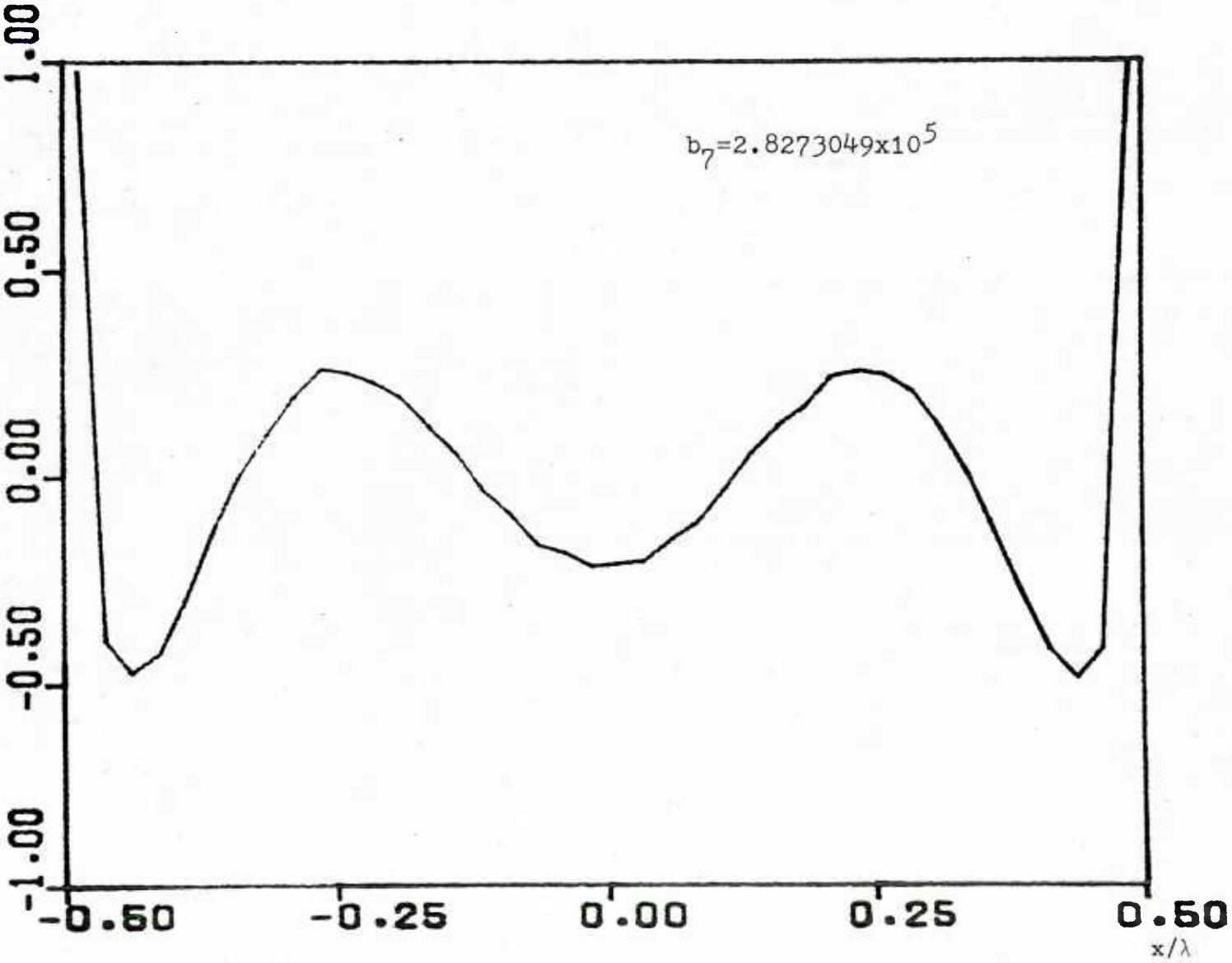

(f)

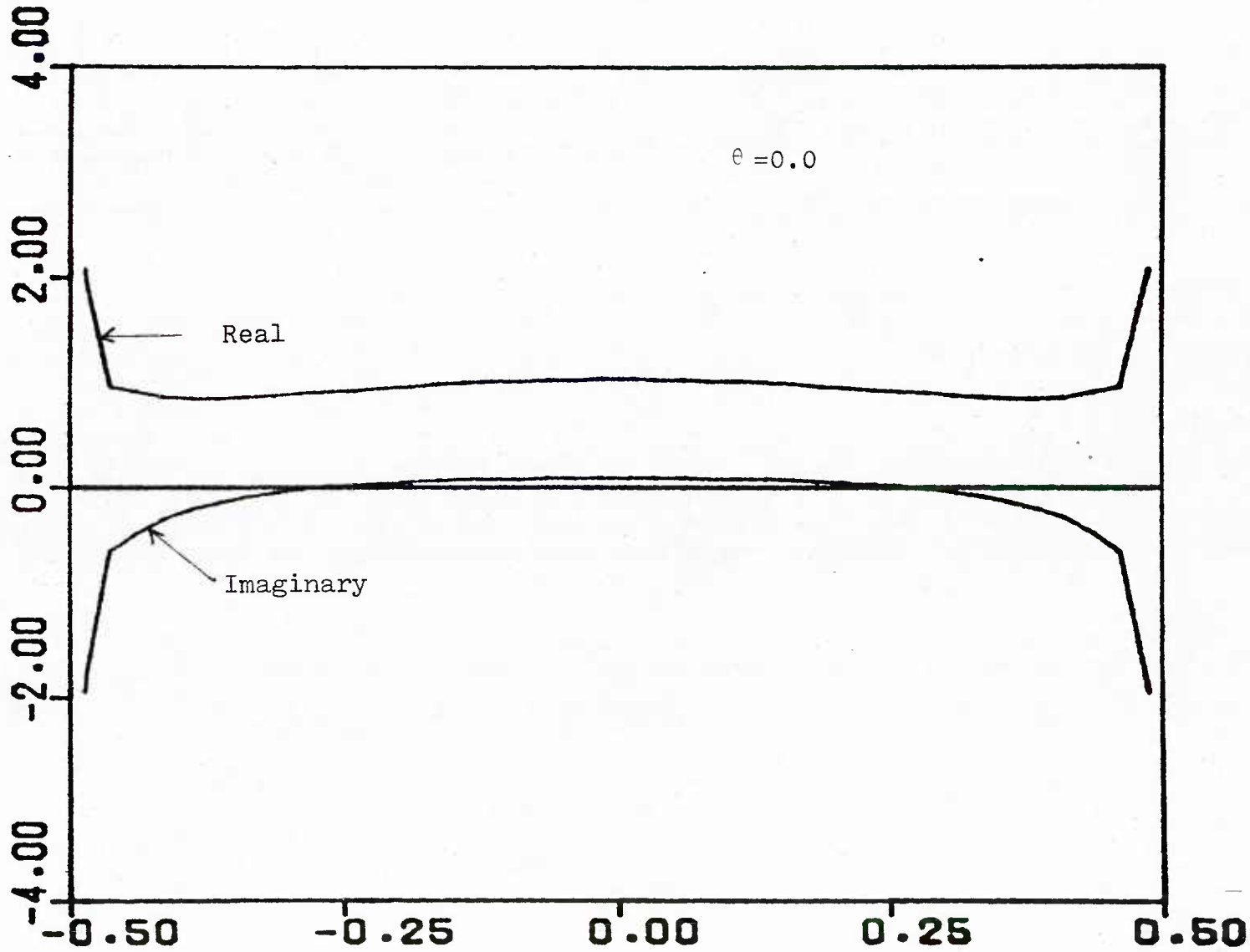

Figure 19: The equivalent magnetic current for a 1.0λ slot. Only the (7) physical characteristic currents are used in the summation.

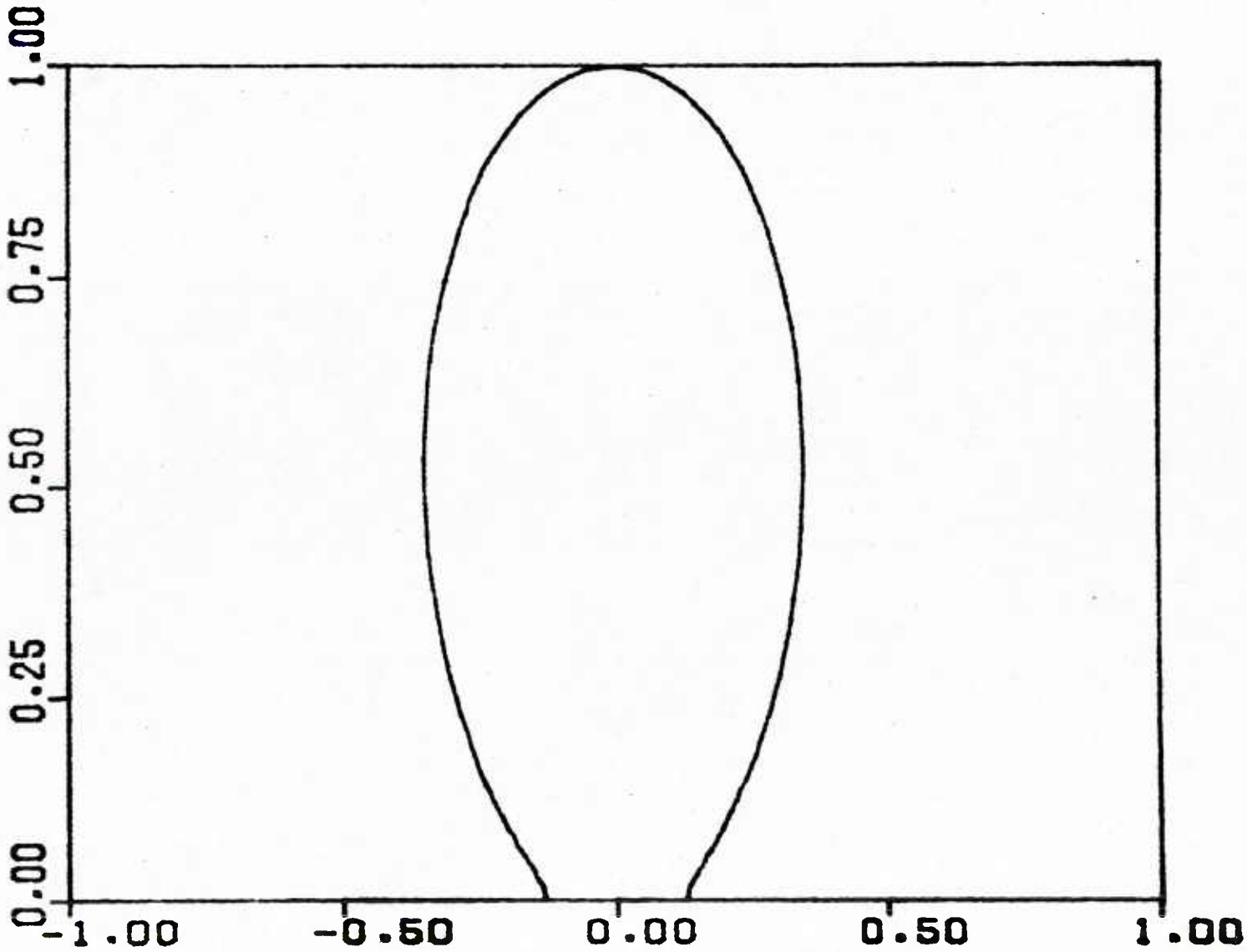

$|\underline{H}_1|$

(a)

Figure 20: The radiation pattern of (a) the first,...,(g) seventh chracteristic fields for 1.0λ slot.

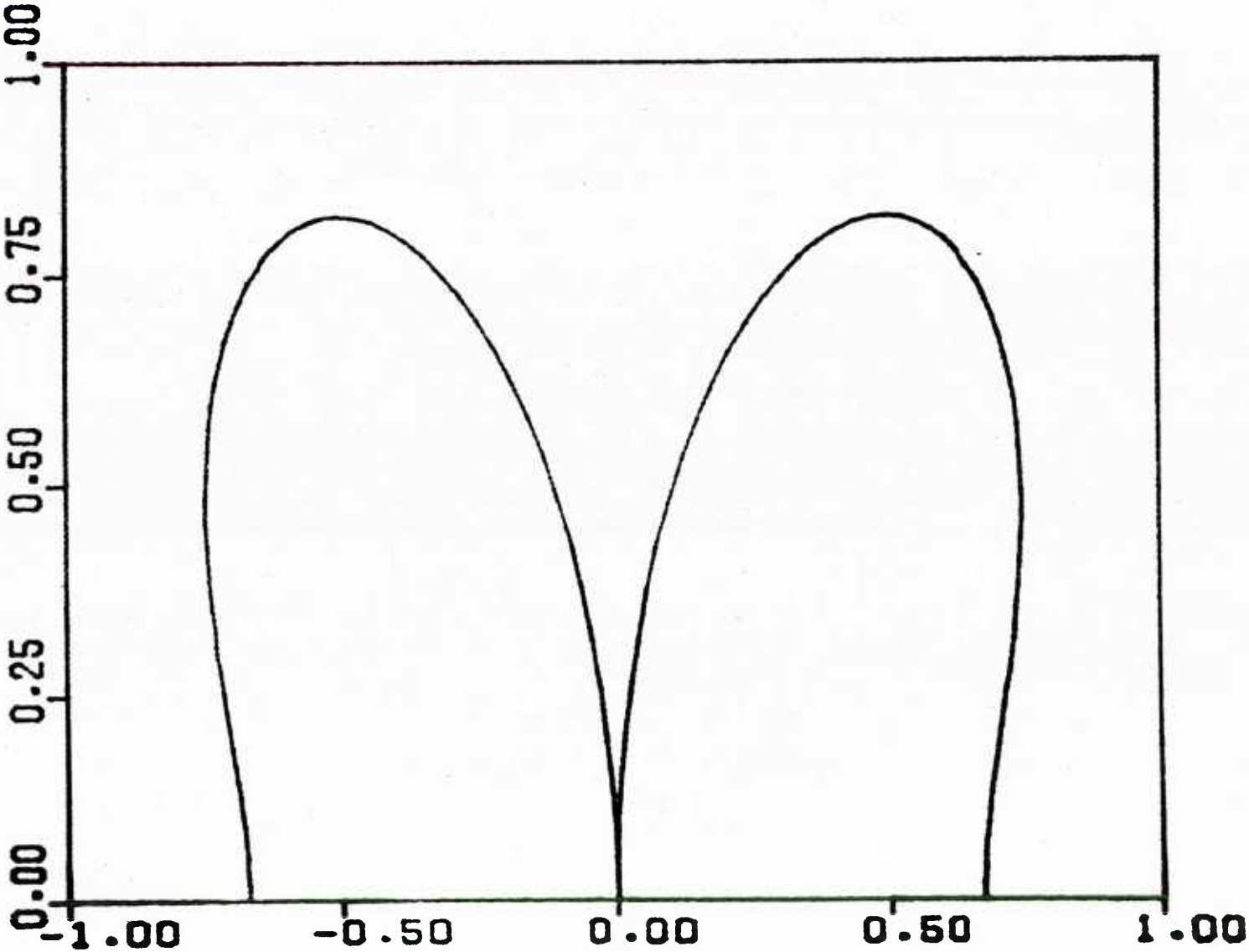

$|\underline{H}_2|$

(b)

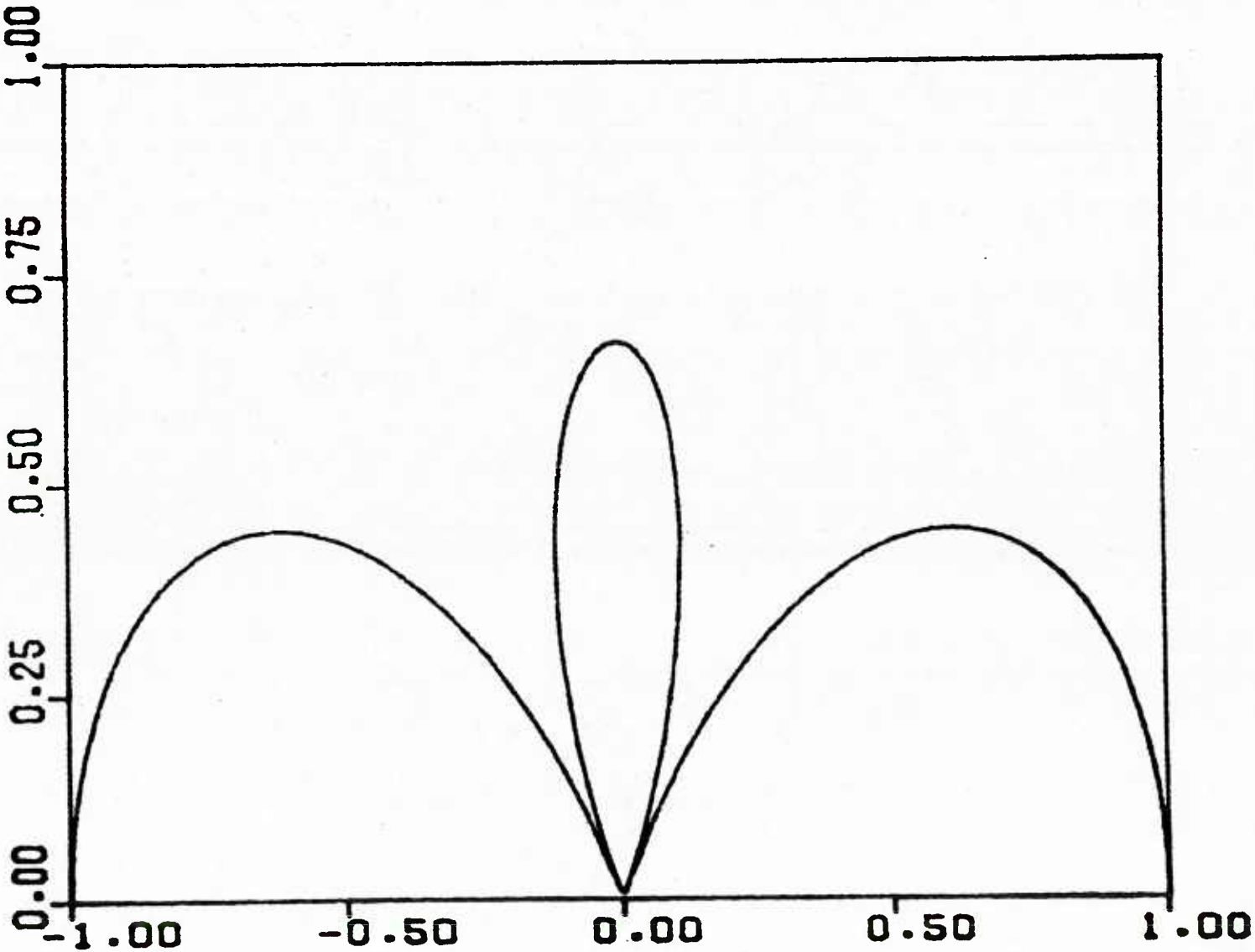

$|H_3|$

(c)

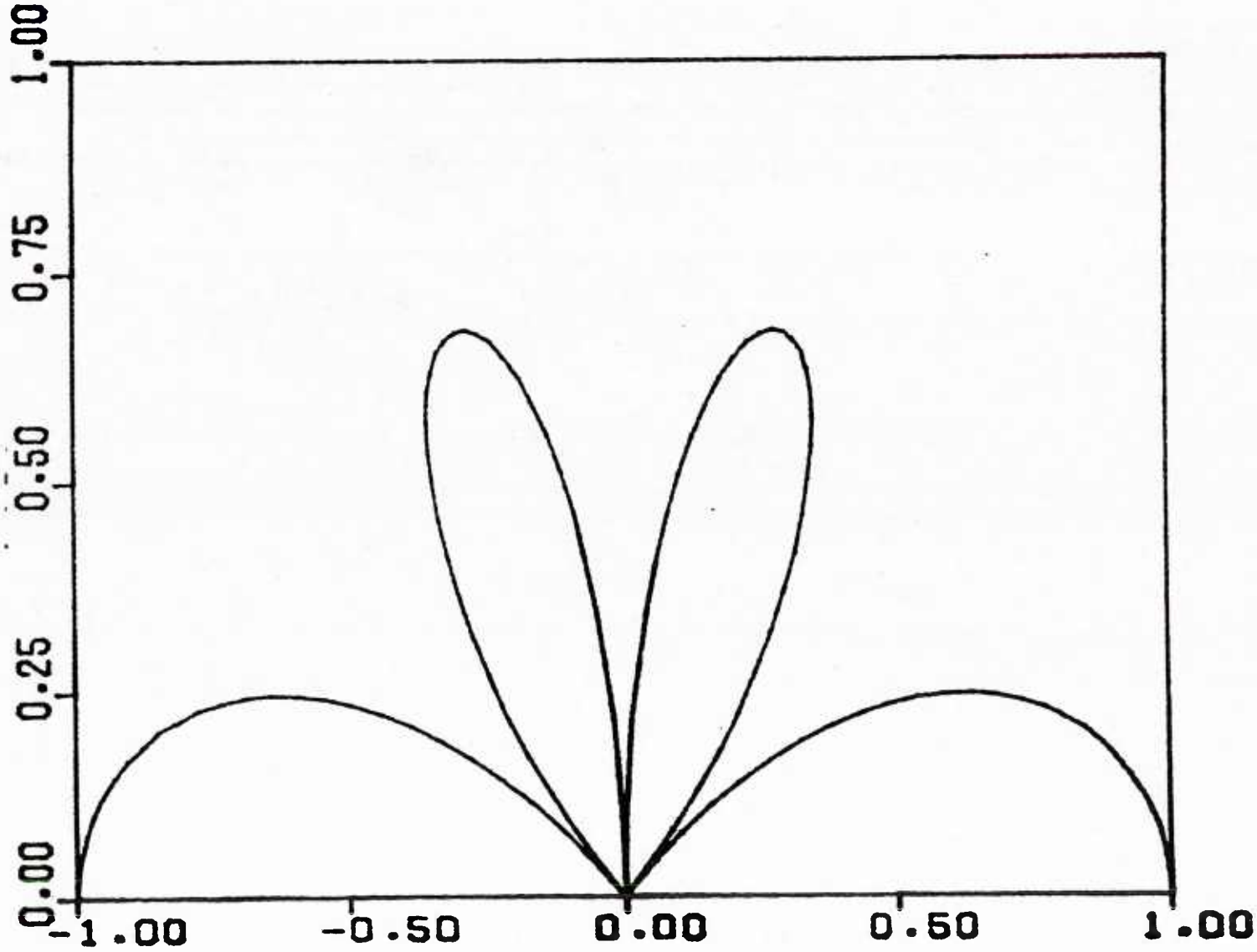

$|\underline{H}_4|$

(d)

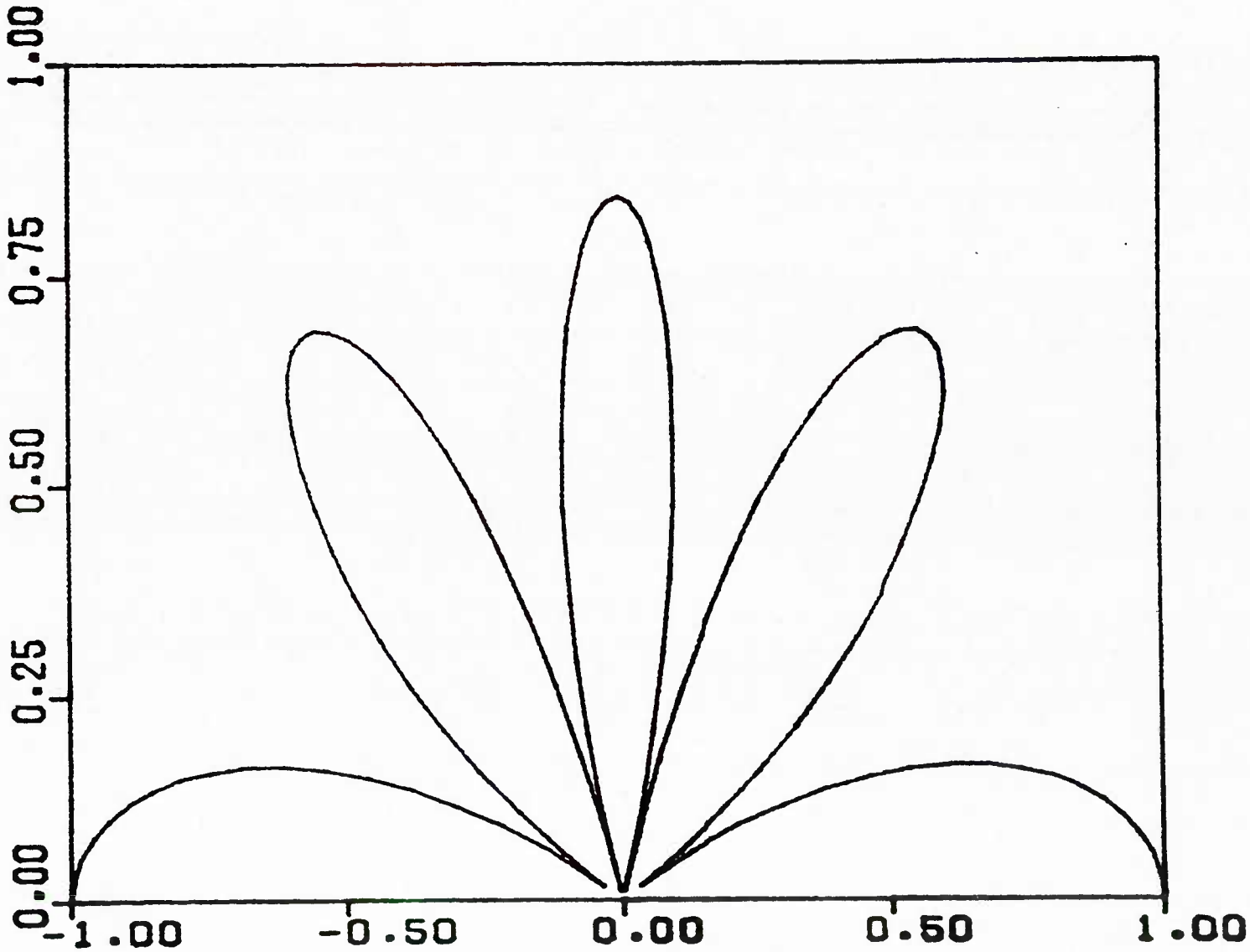

$|\underline{H}_5|$

(e)

$|\underline{H}_6|$

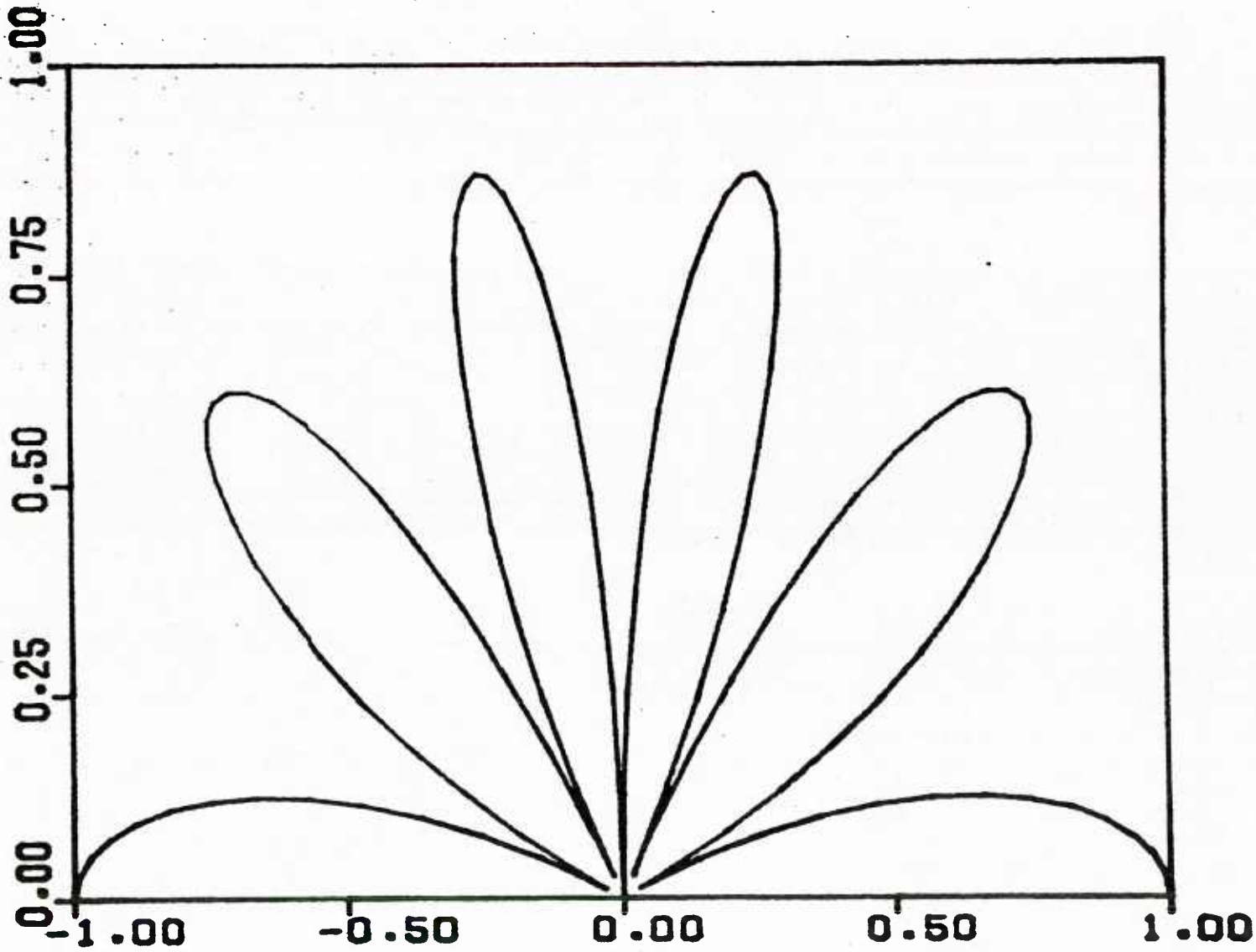

(f)

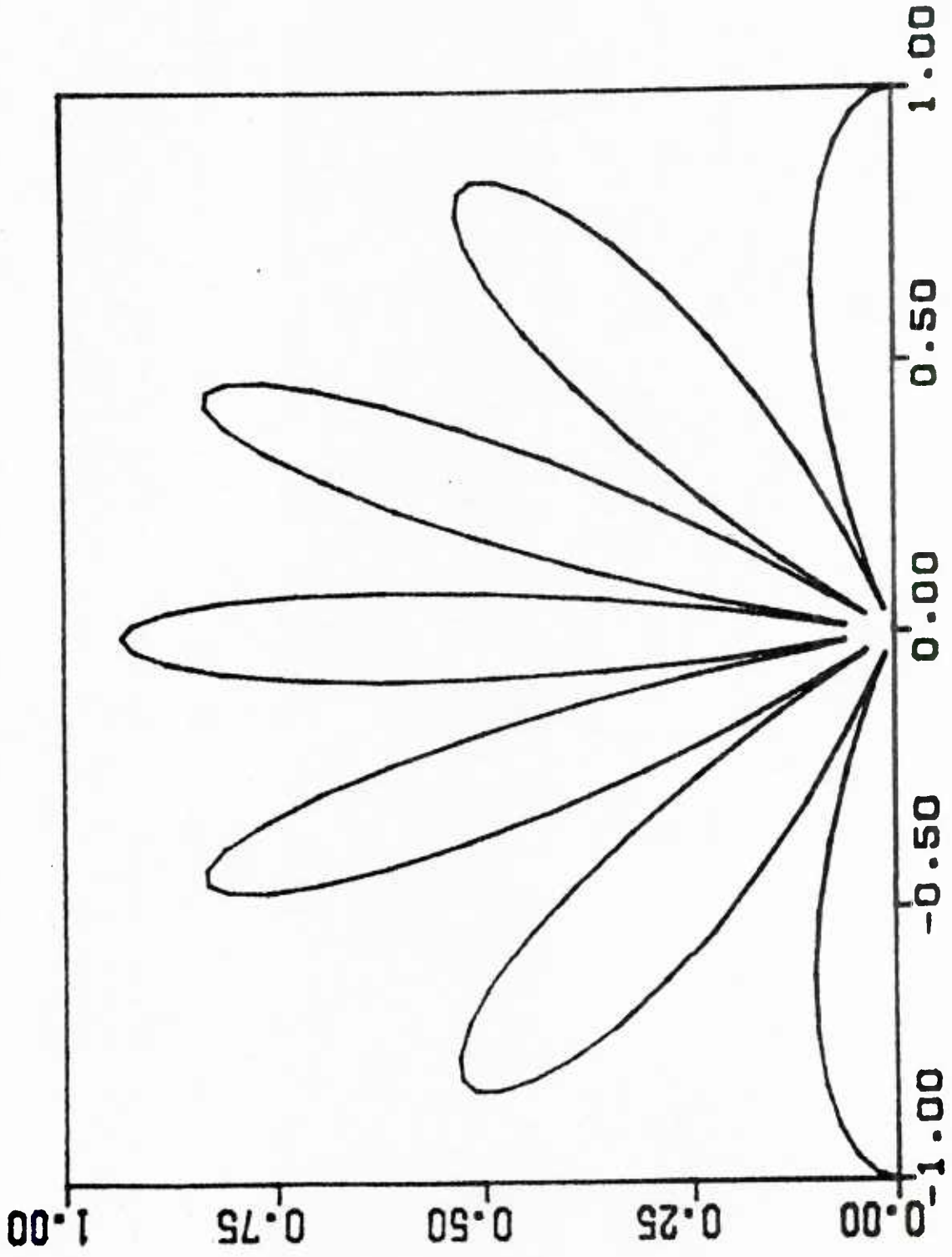

(g)

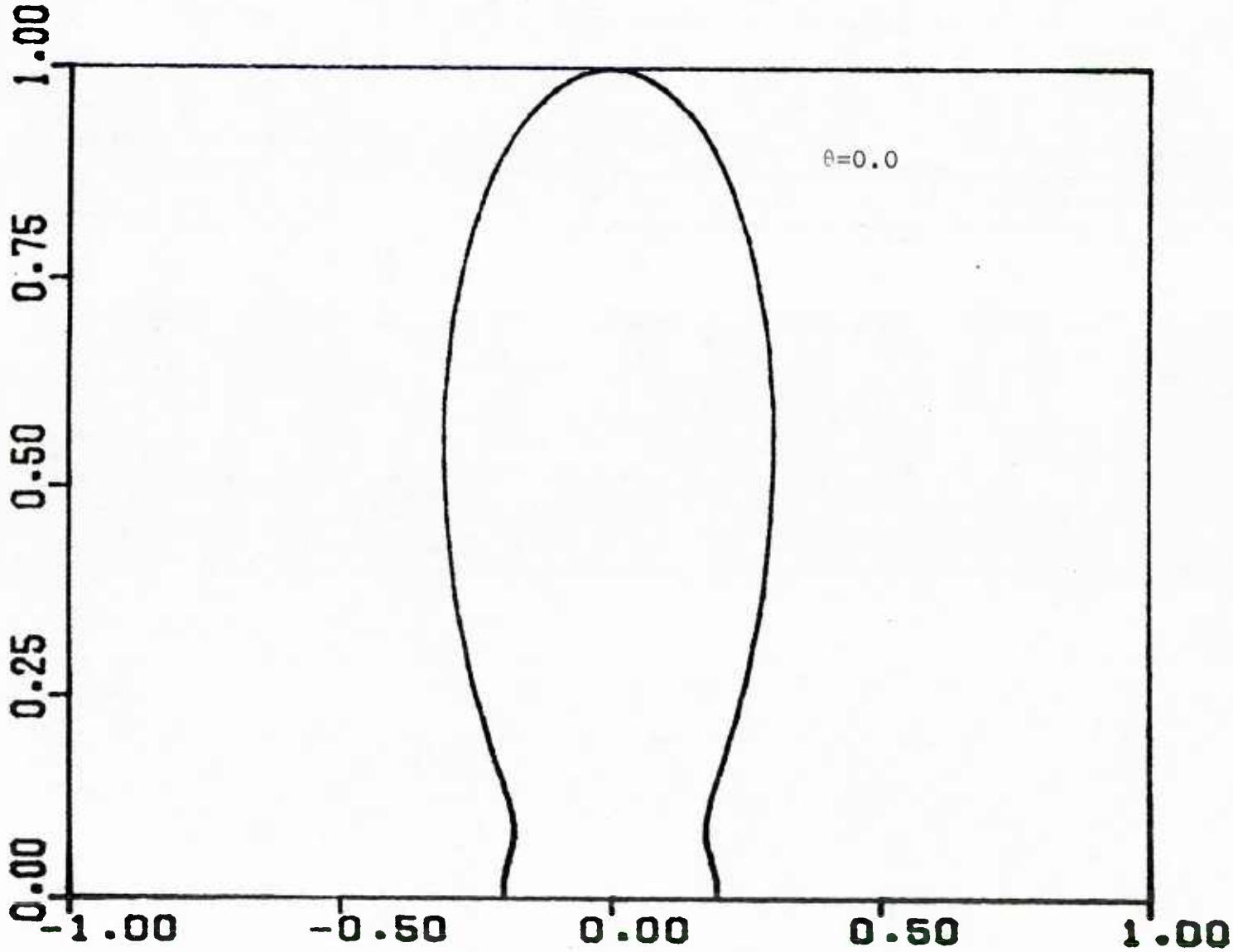

Figure 21: The radiation pattern to a 1.0λ slot.

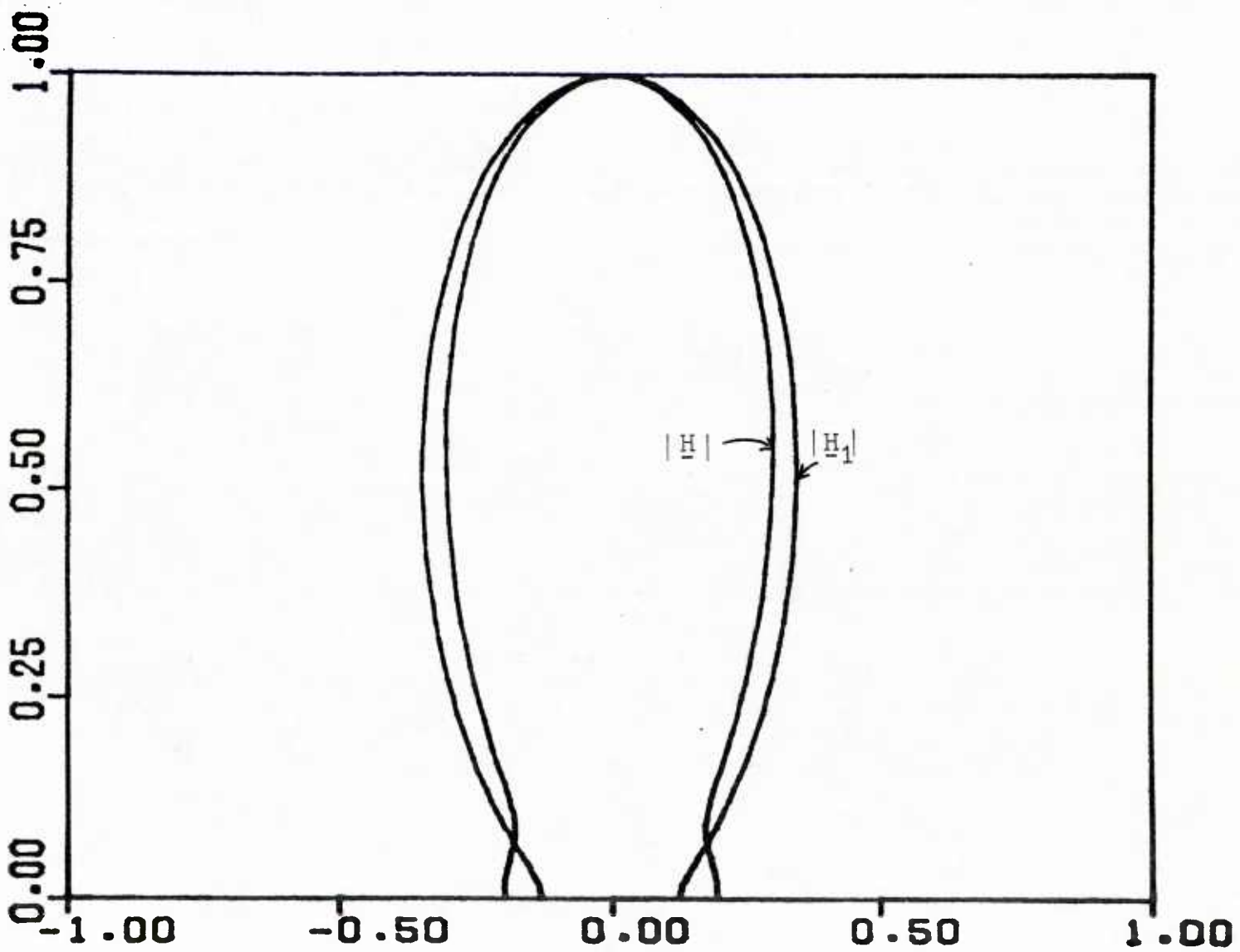

Figure 22: Comparison of the radiation pattern for a 1.0λ slot (θ=0.0) to that of its dominant chracteristic field.

11. Discussion

The theory of characteristic modes for slots has been applied for the solution of the problem of an infintely long slot in a ground plane in an unbounded medium illuminated by a uniform TE (to the slot axis) plane wave. The theory is a specialization of the general theory of characteristic modes for apertures, and can be applied to slots in a ground plane separating contrasting mediums and illuminated by general plane waves.

The characteristic currents and fields, as well as the equivalent magnetic current, transmission coefficient, and radiation pattern, of the slot have been computed for different slot widths. The theory is rather general and computationally efficient, applicable to both narrow and wide slots. For narrow slots, the modal representation of the equivalent magnetic current is readily recognized as an augmented multipole expansion of the cuurent. Furthermore, it appears only a finite number of characteristic currents need to be computed. The applicability of the theory is not necessarily confined to slots of small or intermediate width compared to the wavelength. In fact, it is computationally more attractive than a great many other numerical solutions. This is evident from its performance in the present situation. All the interesting features displayed here are expected to carry through for general apertures and mediums.

Appendix

In this Appendix, it is shown that the convergence of the field

$$\underline{E}(\underline{M}) = \sum_{n} V_n \underline{E}_n \tag{1}$$

over the radiation cylinder is in a least squares sense. The proof for $\underline{H}(\underline{M})$ is similar.

Put

$$\underline{E}(\underline{M}) = \sum_{n=1}^{N} U_n \underline{E}_n + \underline{R}_N(\underline{E}) \tag{2}$$

where

$$\underline{R}_N(\underline{E}) = \sum_{n=1}^{N} (V_n - U_n) \underline{E}_n + \sum_{n=N+1}^{\infty} V_n \underline{E}_n \tag{3}$$

is a residual term. Then, the convergence of $\underline{E}(\underline{M})$ in a least squares sense over the radiation cylinder is equivalent to the requirement that the norm of the residual

$$||\underline{R}_N(\underline{E})||^2 = \int_{Cy_\infty} \underline{R}_N^*(\underline{E}) \cdot \underline{R}_N(\underline{E}) \, d\tau \tag{4}$$

be minimum if and only if $U_n = V_n$, $n=1,2,..,N$. Substituting (3) into (4) and using the orthogonality relationship (31.1), it becomes

$$||\underline{R}_N(\underline{E})||^2 = \frac{\zeta}{2} \left[\sum_{n=1}^{N} |V_n - U_n|^2 + \sum_{n=N+1}^{\infty} |V_n|^2 \right]. \tag{5}$$

The result then follows.

References

[1] R. F. Harrington and J. R. Mautz, "A Generalized Network Formulation for Aperture Problems," IEEE Transactions on Antennas and Propagation, Volume AP-24, Pages 870-873, November 1976.

[2] R. F. Harrington and J. R. Mautz, "Characteristic Modes for Apertures," IEEE Transactions on Microwave Theory and Techniques. To appear.

[3] T. Y. Chou and A. T. Adams, "The Coupling of Electromagnetic Waves through Long Slots," IEEE Transactions on Electromagnetic Compatibility, Volume EMC-19, Pages 65-73, May 1977.

[4] C. M. Butler, Y. Rahmat-Samii, and R. Mittra, "Electromagnetic Penetration through Apertures in Conducting Surfaces," IEEE Transactions on Electromagnetic Compatibility, Volume EMC-20, Pages 82-93, February 1978.

[5] R. F. Harrington, Time-Harmonic Electromagnetic Fields, McGraw-Hill Book Company, New York, New York, 1961.

[6] F. B. Hildebrand, Methods of Applied Mathematics, Prentice-Hall, Inc., Englewood Cliffs, New Jersey, 1965.

[7] R. E. Collin, Field Theory of Guided Waves, McGraw-Hill Book Company, New York, New York, 1960.

[8] R. F. Harrington and J. R. Mautz, "Theory of Characteristic Modes for Conducting Bodies," IEEE Transactions on Antennas and Propagation, Volume AP-19, Pages 622-628, September 1971.

[9] C. M. Butler and D. R. Wilton, "General Analysis of Narrow Strips and Slots," IEEE Transactions on Antennas and Propagation, Volume AP-28, Pages 42-48, January 1980.

[10] R. F. Harrington, Field Computation by Moment Methods, Macmillan Company, New York, New York, 1968. Republished by Krieger Publishing Company, Melbourne, Florida, 1982.

[11] T. M. Apostol, Mathematical Analysis, Addison-Wesley Publishing Company, Reading, Massachusetts, 1974.

[12] M. Abramowitz and I. A. Stegun, Handbook of Mathematical Functions, Dover Publications, New York, New York, 1965.

[13] IMSL Library 2 Manual, 1975.